AD-A124 295 PERFORMANCE OPTIMIZATION OF A PNEUMATIC WAVE ENERGY CONVERSION DEVICE(U) NAVAL ACADEMY ANNAPOLIS MD S W SURKO 26 AUG 82 USNA-TSPR-120 1/1

UNCLASSIFIED F/G 10/2 NL

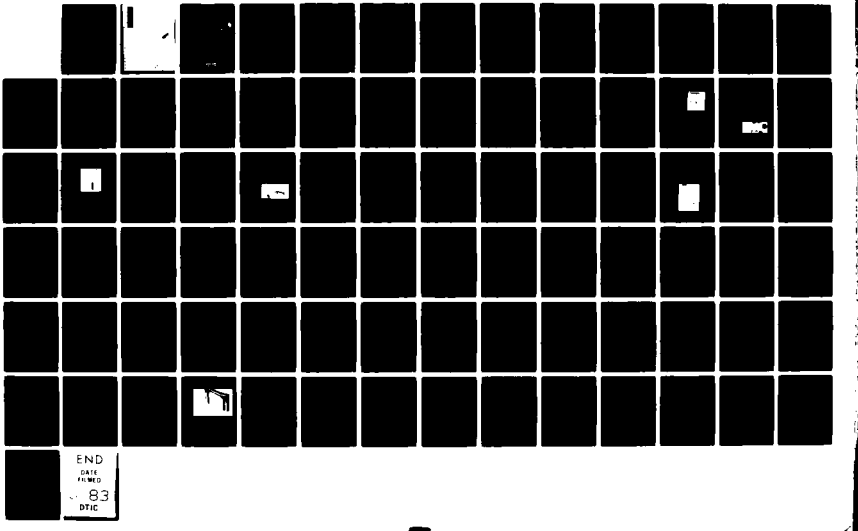

END
DATE FILMED
83
DTIC

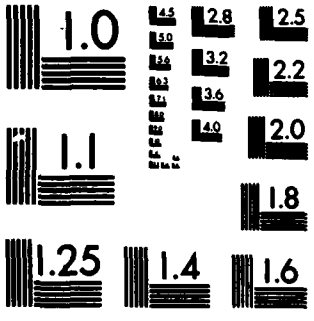

(21)

"PERFORMANCE OPTIMIZATION OF A PNEUMATIC WAVE ENERGY CONVERSION DEVICE"

A Trident Scholar Project Report

by

Midshipman Stephen W. Surko, 1/C
U. S. Naval Academy
Annapolis, Maryland

Michael E. McCormick

Dr. M. E. McCormick
Naval Systems Engineering Department

Accepted for Trident Scholar Committee

Charles Rector

Dr. C. W. Rector, Professor, Chairman

26 Aug 82

Date

To my grandparents, whose service to our nation in World Wars One and Two and very special warmth of character have always been a source of support and inspiration.

ACKNOWLEDGEMENTS

The author would like to express sincerest appreciation to the many people who contributed their time, efforts, ideas, and encouragement:

Dr. M. E. McCormick, Professor, Naval Systems Engineering Dept., U. S. Naval Academy

Dr. B. Johnson, Professor, Naval Systems Engineering Dept., U. S. Naval Academy

LCDR J. W. Patton, Division of Engineering and Weapons, U. S. Naval Academy

Dr. S. Burns, Professor, Electrical Engineering Dept., U. S. Naval Academy

Mr. W. Roloson, Technical Support Dept. Supervisor, Division of Engineering and Weapons, U. S. Naval Academy

Mr. D. Gosewisch, Technical Support Dept., Division of Engineering and Weapons, U. S. Naval Academy

Mr. H. Hoffritz, Technical Support Dept., Division of Engineering and Weapons, U. S. Naval Academy

Mr. T. Price, Technical Support Dept., Division of Engineering and Weapons, U. S. Naval Academy

Mr. J. Hill, Hydromechanics Laboratory, Division of Engineering and Weapons, U. S. Naval Academy

Mr. J. Salsich, Hydromechanics Laboratory, Division of Engineering and Weapons, U. S. Naval Academy

Mr. S. Enzinger, Hydromechanics Laboratory, Division of Engineering and Weapons, U. S. Naval Academy

Mr. D. Bunker, Hydromechanics Laboratory, Division of Engineering and Weapons, U. S. Naval Academy

and also to his classmate, Midshipman C. Calhoun, who took pity on the author's agonizingly slow pecking on the typewriter and offered to help type a few pages. Before her fingers gave out it was past midnight of the day before the report was due, and there was a stack of 25 pages to one side of her typewriter.

ABSTRACT

The performance of a pneumatic wave energy conversion device was optimized by developing resonance within the device's oscillating water column and impedance matching the system.

The pneumatic device investigated was one quarter the size of prototype recently constructed. Within its capture chamber is a column of water which is excited by the incident waves. The capture chamber has a bottom opening so that the system is omni-directional. As the water column oscillates it forces air through a special counter-rotating axial flow turbine developed by Professor M. McCormick which always drives an output shaft in the same direction regardless of the direction of air flow. The internal water column oscillations obey the equation of motion.

In accordance with the equation of motion the author was able to control the internal frequency of oscillation to develop resonance with the incident waves. This resonant condition served to strengthen the oscillations of the water column within the capture chamber and to attract additional wave energy through an effect known as "antenna focusing." In this study, resonance was achieved by varying the length of submergence of the capture chamber.

A special low-rpm generator was purchased to convert the turbine revolutions into useable power. A linkage system consisting of a 10-speed bicycle's chain and gears was modified to transfer the turbine rpm to the generator, and the generator load to the turbine, to impedance match the system. The various gear

ratios allowed the system to be impedance matched for different incident waves.

During monochromatic wave testing a maximum efficiency of 35.6% was achieved, at a developed power of 86.5 watts. Efficiencies dropped off rapidly in wave conditions of less incident power.

During the brief period of random sea wave testing the efficiency dropped as low as .6%, as compared to 10% for a similar monochromatic wave. There appear to be several means of improving the random sea performance. The use of a flywheel to smooth out the turbine response to the varying incident waves was found to offer promise, although the one which the author added on to the turbine was too small to have a significant effect. If, instead of using the submergence length, air compressibility is used to control the internal water column frequency then response to varying incident waves could be swift to maintain resonance. A control system is necessary to adjust the air compressibility and the system load to maintain optimum performance in ocean wave energy conversion revealed by the brief period of random sea testing the great potential for pneumatic wave energy conversion remains.

TABLE OF CONTENTS

I. INTRODUCTION

A. Background

The oceans are a rich and inexhaustible source of energy. Over a century of interest in the oceans has led inventive engineers to patent over 1000 ocean energy conversion devices. This has been particularly so within the last decade's realization that the era of cheap fossil fuels has expired. Ocean energy exists in many forms: tidal, ocean currents, salinity gradients, thermal gradients, and wave power. The most obvious form of energy is the surface wave, which appears to offer the best possibilities for practical ocean energy conversion.

Wave energy is developed through four basic phenomena: (1) bodies moving on or near the surface producing relatively low period waves of low energy; (2) wind generated seas and swells; (3) seismic disturbances producing "tsunamis;" and (4) the lunar and solar gravitational fields causing the longest waves, the tides. From figure 1.1 one notes that tidal and

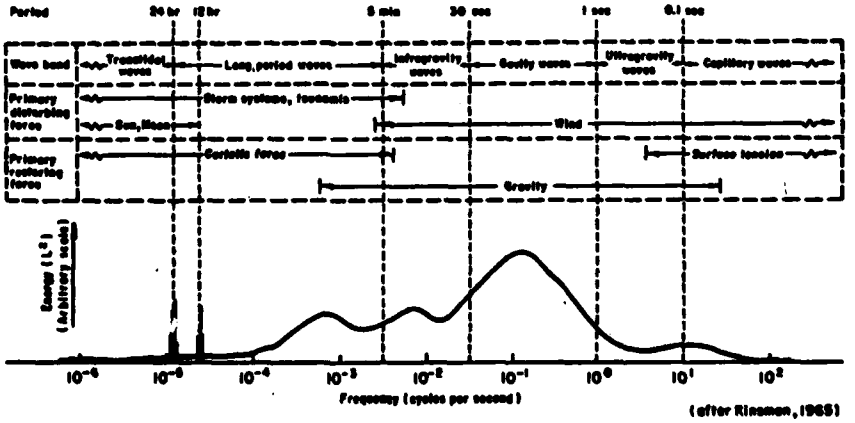

Figure 1.1: Relative ocean wave energies vs. frequency and period.

wind waves possess the greatest amounts of energy. Tidal energy is already being converted into useable power in certain limited coastal areas which possess a large tidal range, such as the Bay of Fundy in Canada. It is interesting to note that wind waves, which can contain enough energy to violently toss around an 8000 ton destroyer, are actually a form of solar energy. Due to the great abundance of wind wave energy, its practical conversion into useable power has been receiving renewed interest.

There are essentially 9 methods of wave energy conversion, which are described in McCormick (1981). They are:

1) Heaving Bodies
2) Pitching and/or Rolling Bodies
3) Pneumatic or Cavity Resonators
4) Focusing Systems
5) Pressure Devices
6) Surging Systems
7) Flaps and Paddles
8) Rotating Outriggers
9) Combination of the above

The most contemporary application of one of these methods was due to the efforts of Masuda of the Japan Marine Science and Technology Center and R. M. Ricafranca of RMR Research and Engineering Services in the Philipines. These two investigators, working independently, were responsible for the first wave energy conversion systems designed to provide power for navigation aids such as light buoys. They used the pneumatic or cavity resonating method.

It was the same general pneumatic resonating concept which was investigated in this study. The pneumatic wave energy conversion device that this author worked with acted as a single-degree-of-freedom system having only vertical motions (see Figure 1.2).

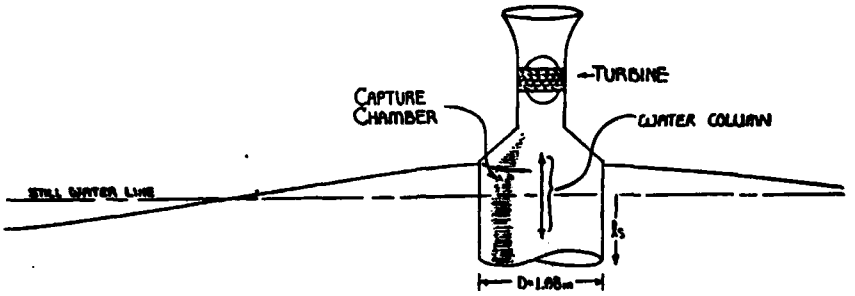

Figure 1.2: Pneumatic wave energy conversion device profile. A wave front passing the device forces the column of water within the capture chamber to oscillate like a piston, forcing air through a special counter-rotating axial flow turbine patented by Professor M. McCormick. The output of the turbine drives a generator, thus producing useable power.

B. Purpose of Study

The purpose of this study was, for the first time, to optimize the performance of a pneumatic wave energy conversion device. The experiments of Jolly and Newmaster (1979) and Trop and Casey (1980) left a capture chamber and turbine for further investigation. There had been no attempt to attach a generator to the turbine to produce electrical power. Trop and Casey developed a maximum of 2.45 watts from the turbine, and an efficiency of 6% in small waves of under 7 inches incident upon the capture chamber. To optimize the system →

performance the turbine had to be first analyzed so that its power performance curves could be determined. These curves were needed to help define the possible overall performance of the system, and for the impedance matching of the system necessary for performance optimization. The airflow throughout the system had to be smoothed out and the turbine needed to be strengthened. Amplification of the water column oscillations within the capture chamber had to be determined for undamped and various damped operating conditions to simulate the effect of adding the turbine assembly to the capture chamber during later testing. With this knowledge, an appropriate generator was purchased and a generator-turbine linkage designed and built. The completed system was then analyzed in the 380 ft wave tank at the U. S. Naval Academy to establish its optimum performance. → p 41

II. WAVE MECHANICS

A. Linear Theory

As all wave energy devices depend upon the performance of the waves it is vital to understand those waves. A wave is energy in transition as it moves away from its source. The source is generally found to be out at sea above the deep water where various trade winds act, and it is in deep water where the wave energy is at its greatest. Budal and Falnes (1974) state that the average power in the deep water of the North Atlantic is roughly 60 kW/m of crest length. The available power in deep waters off the coast of the Pacific Northwest are of the same order of magnitude, from McCormick (1981). As a wave approaches shore it interacts with the sea floor and loses energy due to bottom friction and irrotationalities.

The deep water condition is an important concept. A wave in deep water is unaffected by the sea floor beneath it. The simple relationship

$$d = \frac{\lambda}{2} \qquad 2.1$$

defines the deep water condition, with d representing depth and λ representing wavelength. Deep water waves can be accurately represented by the linear sinusoidal wave theory, shown in Figure 2.1 on the following page. According to the linear theory, individual waves travel at a phase velocity, C, where

$$C = \frac{\lambda}{T} = \frac{gT}{2\pi} \text{ TANh}(Kd) \qquad 2.2$$

and where K is the wave number defined by

$$K = \frac{2\pi}{\lambda} \qquad 2.3$$

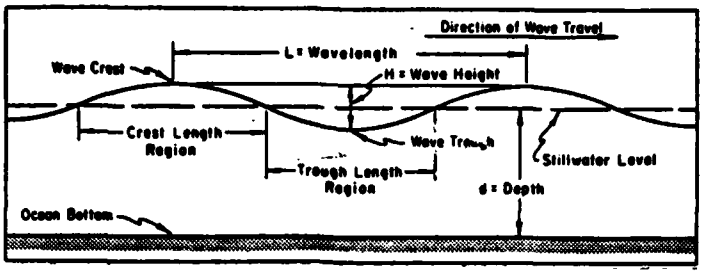

Figure 2.1: Linear (sinusoidal) wave profile.

When the depth becomes less than half the wavelength the wave begins to "feel" the bottom. As it approaches shore the period remains constant, the wavelength decreases and the wave height increases, as shown in Figure 2.2 below.

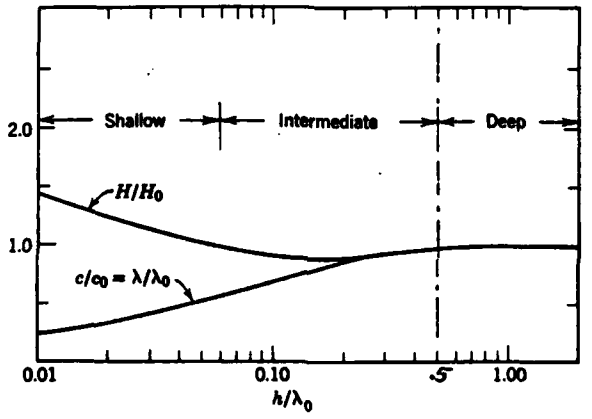

Figure 2.2: Dimensionless wave properties as functions of the depth of deep water wavelength ratio as predicted by the linear theory.

Although several nonlinear wave theories are used to more accurately describe the wave motions in shallow water, the linear theory is the accepted theory for deep water and even some intermediate water analysis due to its accuracy and simplicity of use.

As derived by McCormick (1973) and others the total energy in a wave is obtained from

$$E = \frac{\rho g H^2 \lambda b}{B} \qquad 2.4$$

where b is the width of the crest, and H is the wave height. The transfer of energy from one point to another (the energy flux) is characterized by the wave power

$$P = \frac{\rho g H^2 Cgb}{B} \qquad 2.5$$

where Cg is the group velocity, depicted in Figure 2.3 below

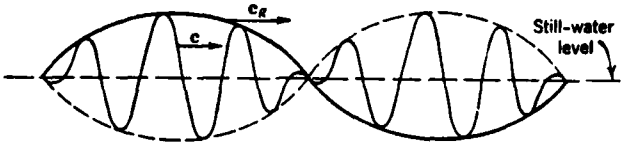

Figure 2.3: Wave group profile

and represented be

$$Cg = \frac{C}{2}\left[1 + \frac{2Kd}{SINh(2Kd)}\right] \qquad 2.6$$

When a group of waves is observed traveling in deep water the waves appear at the rear of the group and move to the front, and then disappear. Thus in deep water the group velocity becomes

$$Cg = \frac{C}{2} \qquad 2.7$$

In shallow water one finds that

$$Cg = C \qquad 2.8$$

B. Random Sea

The wind is the direct energy source of most ocean waves. The wave height, period, and direction are thus related to the velocity, direction, and duration of the wind. A mild breeze will generate waves of small height and low period that generally propogate in the direction of the wave. Storm-generated seas on the other hand include waves of various heights and periods that travel in many directions. Such a

condition is known as a random sea, but can in reality be considered to be a composition of numerous linear waves of various heights and periods, each traveling in a particular direction, according to McCormick (1981). As most wave energy conversion devices are frequency dependent since they operate most efficiently at their own natural frequency, their efficiency in an actual (random) sea will be slightly less than in a monochromatic or single-frequency sea.

C. Wave Modification

The interactions of the wave with the bottom, the shore, and with the structure are very important. It is desirable to modify the wave motions to improve the performance of the device. A water wave can be redirected in the following three manners: (1) refraction; (2) reflection; and (3) diffraction. Both refraction and reflection are important concepts to apply to performance optimization of a pneumatic wave energy conversion device.

As a wave front approaches shore and enters intermediate water it will begin to "feel" the bottom. The wave front will bend according to Snell's Law

$$\frac{\text{SIN } B}{\text{SIN } B_0} = \frac{C}{C_0} = \frac{\lambda}{\lambda_0} \qquad 2.9$$

where B is the angle between the wave front and the depth contour within the shoaling region and B_0 is the angle between the deep water wave front and the first shoaling contour. The effect of refraction upon the wave height is obtained from the expression

$$H = KsKrHo \qquad 2.10$$

where Ks is the shoaling coefficient, defined by

$$Ks = \left(\frac{Cg_0}{Cg}\right)^{1/2} = \frac{H}{H_0'}, \qquad 2.11$$

where the wave height H_0' is that of the deep water wave if no refraction had occured in the shoaling. The refraction coefficient, Kr, is defined by

$$Kr = \left[\frac{\cos(B_0)}{\cos(B)}\right]^{1/2} \qquad 2.12$$

The importance of this is that a mound on the sea floor, either man-made or natural, could be used to act as a "lens" and direct or focus additional wave energy towards the pneumatic conversion device or devices (see Fig. 2.4)

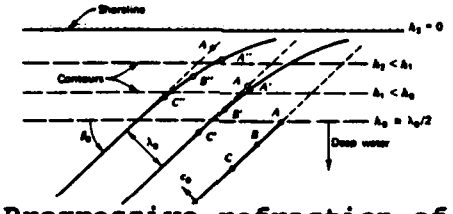

Figure 2.4: Progressive refraction of a shoaling wave

An artificial submerged "atoll" around a device would produce "island" focusing.

The pneumatic wave energy conversion device investigated in this study acts as a point oscillator producing dynamic reflection with the incident waves, according to Falnes and Budal (1978). The radiated waves from the capture chamber, when its water column is oscillating in resonance with the incident waves causing "antenna" focusing of the incident wave energy upon the resonating device. The optimum power for a single-degree-of-freedom point oscillator thus becomes

$$P_{opt} = \frac{P\lambda}{2\pi b} \qquad 2.13$$

where P is the wave power per unit crest length as given in equation 2.5. The antenna focusing effect draws in wave energy from a width of $\frac{\lambda}{2\pi}$, as shown in Figure 2.5 below.

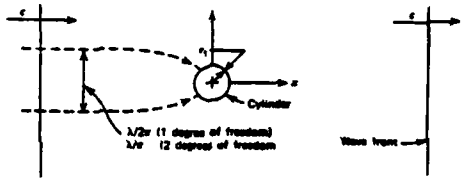

Figure 2.5: Areal sketch of focused wave power. For practical extraction of large quantities of wave energy a row of point oscillators acting in unison would be used (see Fig. 2.6). The optimum wave power available to any given device would then become

$$P_{opt.} = \frac{P\ell COS(B)}{2b} \qquad 2.14$$

which is a function of the incident wave angle B to the row. This only holds true if the separation length ℓ is

$$\ell \leq \frac{\lambda}{\pi COS(B)} \qquad 2.15$$

If the separation length becomes greater the devices would act as individual point oscillators and a certain amount of wave energy would pass undisturbed between the devices.

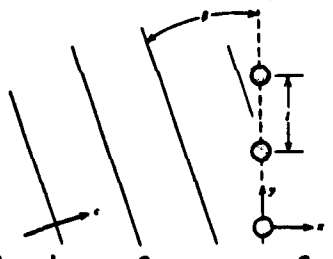

Figure 2.6: Areal view of a row of pneumatic devices.

The optimum power would occur when the wave front was alligned with the row of pneumatic devices, producing

$$P_{opt.} = \frac{P\lambda}{2\pi b} \qquad 2.16$$

It is thus possible for a row of oscillating devices to effectively capture the incident wave energy without reducing the efficiencies of the individual pneumatic devices.

III. MECHANICS OF A PNEUMATIC WAVE ENERGY CONVERSION DEVICE

The principal driving component of a single-degree-of-freedom pneumatic device is the oscillating water column within its capture chamber. The capture chamber has a bottom opening so that the system is omni-directional. Although front facing openings improve the efficiency of the device, since the water column motions are excited by the total wave pressure rather than solely the changes in static pressure, they also limit the placement of such a device. To be effective, such a device would normally be used in a coastal zone which experiences a steady presominant wave direction, but whose waves had already lost most of their energy. Even though it is limited to an efficiency of 50% since it only converts kinetic wave energy the omni-directional opening is ideal for deep water and its inherently greater energy resources.

The vertical motions of the water column satisfy the equation of motion

$$m + a(w)\ddot{z} + b(w)\dot{z} + cz = F(w,t) \qquad 3.1$$

where m=water column mass

$a(w)$ = added-mass effect of an oscillating water column

$b(w)$ = damping

c = restoring force

$F(w,t)$ = external wave force

z = vertical displacement of the water column, with the "dots" referring to time-differentiation

From McCormick (1981) it is possible to define many of the quantities in the equation of motion, which makes it possible to see how the water column oscillations can be controlled to achieve optimum performance.

The mass of the cylindrical water column in a dead calm is

$$m = \rho \pi D^2 \ell s/4 \qquad 3.2$$

The added-mass expression reduces to

$$a(w) = \rho \frac{D^3}{3} \left[1 - \frac{1.3K^3D^3}{15} + \frac{K^4D^4}{525} \right] \qquad 3.3$$

The system damping, b(w), consists of three components: (1)viscous; (2)radiation; and (3)extraction of useable energy

$$b(w) = Rv + Rr(w) + Re(w) \qquad 3.4$$

As the viscous resistance is negligible, the relationship becomes

$$b(w) = Rr(w) + Re(w) \qquad 3.5$$

The optimal value of extraction for maximum power production occurs when

$$Re(w) = Rr(w) \qquad 3.6$$

This is known as impedance matching. The radiation resistance is defined by

$$Rr(w) = \rho \frac{\pi K^2 D^4}{32} \left[1 - \frac{K^2D^2}{24} \right] \left(\frac{g}{K} \text{ TANh } Kd \right)^{\frac{1}{2}} e^{-K\ell s} \qquad 3.7$$

To maintain proper impedance matching is a random sea a feedback control system would be necessary.

The restoring force, C, consists of a hydrostatic component and a term due to the compressibility of air, Ka. For a circular water column the restoring force becomes

$$C = \rho g \pi D^2/4 + Ka \qquad 3.8$$

An important aspect of performance optimization is controlling the capture chamber's natural frequency of oscillation to match that of the incident external waves. This condition, known as resonance, has several benefits. First, it increases the motions of the water column. In an undamped case at resonance the internal motions are actually greater than the external. And secondly, resonance produces an effective "antenna" focusing effect which increases the wave energy incident upon the device. The internal water column oscillations will resonate with a frequency

$$Wn = \sqrt{\frac{\rho g \pi D^2/4 + Ka}{m + a}} \qquad 3.9$$

where Ka is a "spring constant" due to compressibility of the air. But assuming incompressibility of the air flow, the natural frequency can be rewritten in the following form

$$fn = \frac{Wn}{2\pi} = \frac{1}{Tn} = \frac{1}{2\pi}\sqrt{\frac{g}{\ell s + \ell s'}} \qquad 3.10$$

where ℓ_s is the still water length of the water column (the length of submergence), and ℓ_s' is the added "effective" length due to the added mass excited by the water column oscillations. Thus, the internal natural frequency can be "tuned" to that of the incident waves by adjusting the submergency length. It is also desirable to know roughly what the velocity of the air flow through the turbine is to define one of the design criteria of the turbine such that it could handle the air flow. Assuming incompressibility of the air flow, the continuity equation provides the simple relationship

$$V_2 = V_1 \frac{A_2}{A_1} \qquad 3.11$$

where condition 1 refers to the capture chamber cross section, and condition 2 refers to the turbine cross section. Recent studies have shown that the air can not be considered incompressible, McCormick and Burcher (1982) and others. The general effect of this finding is positive, for it expands the possibilities for matching the frequencies.

IV. THE TURBINE AND GENERATOR ASSEMBLY

A. The Counter-Rotating Turbine

There are two basic turbine configurations which have been explored for converting wave energy into mechanical energy in a pneumatic device. The concept used by the British and the Japanese in the Kaimei study relied upon rectifying flaps or valves to insure uni-directional flow past a "conventional" turbine. This concept introduces the possibility of failure due to fouling causing a flap or valve to jam. This drawback was revealed in the Kaimei study where 27 flap failures occured. The alternative concept has been to design a bi-directional turbine. Such a turbine would be free from the mechanical problems associated with the use of rectifying flaps or valves and would be able to convert energy from the full cycle of the wave.

McCormick (1981) designed an axial flow, counter-rotating bi-directional turbine which requires no rectifying flaps or valves. The concept of the turbine is fairly simple (as shown in Fig. 4.1). The outer vanes are fixed and direct the air flow into the two counter-rotating rotors between them. The rotors always rotate in their own (and opposite) directions regardless of direction of air flow through the turbine. The rotors turn a central shaft system composed of a solid shaft from one rotor going through a hollow shaft attached to the other rotor. The central shaft system rotates the output shaft through the use of gears. The turbine was

used in the pneumatic wave energy conversion device in this study. The turbine was built of wood and enclosed in a plexiglass casing within a long plexiglass tube, as shown in Figure 4.1 below.

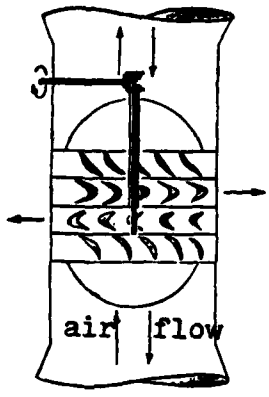

Figure 4.1: McCormick counter-rotating axial flow turbine.

A long period of wind tunnel analysis of the turbine alone was conducted to define its individual performance characteristics. This testing was performed in two phases. During the first phase the turbine built by Trop and Casey (1980) was used. A controllable torque, or load, was provided by the use of a wooden lever-arm attached to the turbine output shaft. Tightening the arm around the shaft increased the applied torque, and directly increased the force which the lever-arm applied to a voltage potentiometer located a specific distance (6 inches) from the turbine output shaft, accurately determined from the relationship

$$T = Fd \qquad 4.1$$

where F is the applied force, and d is the distance from the shaft. A rpm meter was also attached to the turbine output shaft. The torque potentiometer and rpm voltages were fed into a computer program (see Appendix I) which the author modified for this purpose. Calibrations of the voltages produced by the torque lever-arm and the rpm showed linear relationships which simplified the computer's conversion of the voltages into the actual torque applied and resultant rpm at a given air velocity. The program also calculated and printed the power developed by the turbine according to the relationship

$$f = T\Omega \qquad 4.2$$

where Ω is rotations in radians/second.

A jet diffuser was attached to one end of the device to reduce air turbulence at the entrance/exit. The turbine was then sealed to the end of an aerodynamic laboratory wind tunnel, and the air was sucked through the turbine (see Figure 4.3). During each test run at a select air velocity and

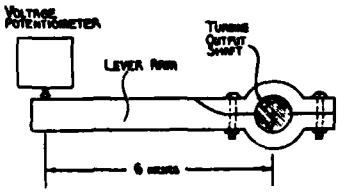

Figure 4.2: Lever-arm

Figure 4.3: Initial turbine set up.

applied torque the program caused the computer to take 10 instantaneous readings of the voltages, average them, and then print out the desired data (see Appendix II). As the changes in air pressure were found to be indiscernable, the air flow velocity was measured with the use of a KERNCO Anemometer. The air flow (and its corresponding velocity) was controlled by placing wooden slats into the wind tunnel to reduce the air flow by various amounts depending upon the amount of air flow obstructed.

The minimal air velocities provided by the small wind tunnel were ideal for simulating the lower air velocities expected to be created by wind waves passing the capture chamber. Turbine performance was evaluated at several air velocities (1.56, 1.92, and 2.23 m/s), and their performance curves were then determined (see Appendix III, and Figures 4.4 and 4.5). The power produced by the turbine increased dramatically with a small increase in the air velocity, as did the applied load. It should be noted that the air velocities specified for the performance curves refer to the stand-still air velocity (with the turbine rotors secured). An investigation of the effect of the spinning rotors upon the air flow revealed that the greater the rpm the greater the "effective" obstruction caused by the revolutions, and the less the actual air velocity became (see Appendix IV).

During wind tunnel testing at a slightly greater air velocity the turbine experienced severe mechanical problems.

The gears slipped and began to strip, the hollow shaft broke free from its rotor, and the turbine output shaft ceased to rotate when the torque (load) was increased to secure the turbine to determine the stand-still air velocity. As these failures indicated the inability of the turbine to handle the greater stresses expected to be produced by any strong wind generated sea to be simulated in the later wave tank analysis, the author decided to rebuild, as opposed to simply repair, the turbine. During the rebuilding process, all the turbine blades were examined for chips and were either filled in or replaced. The internal shaft system was replaced by larger and stronger steel shafts, which made the rotor to shaft attachments more secure, and which when combined with the use of larger ball bearing rings served to stiffen the turbine against the effects of internal twisting caused by the counter rotating rotors. Larger steel gears replaced the stripped brass gears, and the output shaft was also replaced by a larger steel rod. The edges of the internal plexi-glass turbine casing was rounded off to reduce turbulence in the air flow. The turbine was now ready for the second phase of wind tunnel testing.

After it was rebuilt it was important to perform further wind tunnel testing upon the turbine to see if the larger and heavier parts had increased the internal friction of the system, and to see if the turbine could handle the effects of greater air flow. For this series of tests the turbine

was placed over a vertical wind tunnel table (see Fig. 4.6) which had the capability of vertical controlled air flow. This offered the advantage of allowing the turbine to be in a vertical position as it would be on the capture chamber.

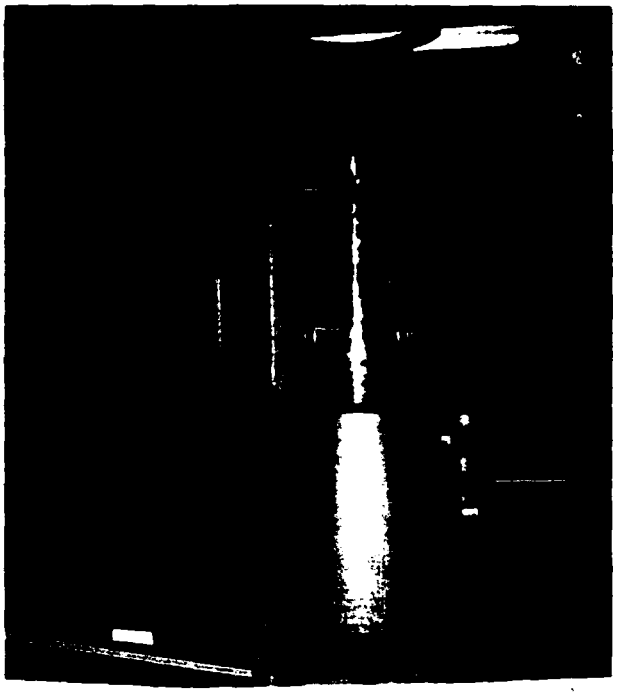

Figure 4.6: Vertical set up for second phase testing.

Several performance curves were developed during this second phase of wind tunnel testing. These curves (at air velocities of 1.18 and 2.75 m/s) are shown on Figures 4.4 and 4.5 along with the first phase curves. It appears that the rebuilding process actually improved the performance of the turbine. Any increase in internal friction was more than compensated for by the more effective repaired blades, smoother internal mechanics, and a smoother and vertical

air flow. In addition to its improved performance was its increased capability to handle greater air flows.

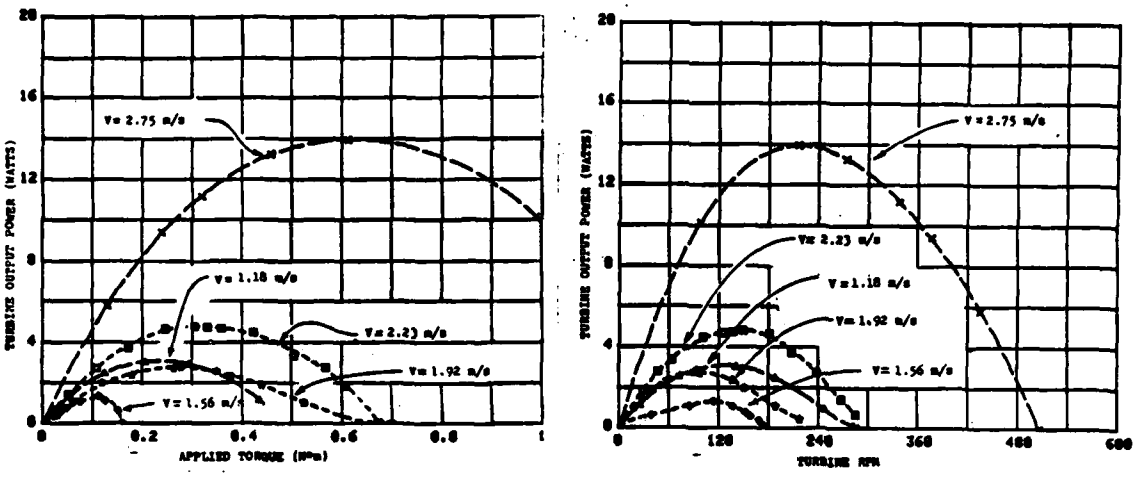

Figures 4.4 and 4.5: Pneumatic turbine performance curves.

B. The Low RPM Generator

The most efficient power output would occur when the frequency of oscillation of the air column equals the wave frequency, and when the extraction resistance equals the radiation and viscous resistance of the water column. Since the extraction resistance is directly related to the applied load it can be controlled. The optimum applied load for the capture chamber is not necessarily the exact same as the optimum applied load for the turbine alone. A generator (the load) had to be chosen which operated in the optimum torque range defined by both the wind tunnel analysis of the turbine and the theoretical radiation resistance defined by equation 3.7.

The generator chosen for the conversion of the turbine's mechanical energy into useable power was the TC25G generator

produced by Thermax Corporation. It is a high-efficiency permanent-magnet dc generator, especially designed for low-rpm renewable energy applications (see Appendix V). The internal resistance of the generator is 7 ohms. The theory of impendance matching also applies to producing optimum power with the generator. Electrical impendance matching was achieved by placing a 7 ohm resistor in series with the generator. A voltmeter was placed in series with the generator and the external resistance (see Fig. 4.7).

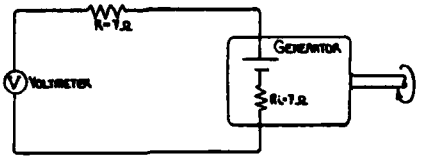

Figure 4.7: Schematic of the generator set up.

The power actually delivered by the pneumatic wave energy conversion device through the generator was measured through the relationship

$$P=\frac{V^2}{R} \qquad 4.3$$

where V is the measured voltage, and R is the 7 ohm external resistance.

C. The Turbine-Generator Linkage System

The optimum extraction resistance for successful impedance matching has to carefully account for its impact upon all phases of the system. Although the TC25G generator operated in the correct low-rpm region it by no means automatically impedance matched the system for optimum

performance. A method was needed to vary the load of the generator upon the system so that the correct load for optimum performance of the device in various sea conditions could be experimentally defined.

A 10-speed bicycle's chain and gear system was adapted for use as the linkage between the turbine and the generator. Such a system (see Fig. 4.8) offered several advantages: (1) inexpensive; (2) low friction in the chain and around the gears would efficiently transfer the turbine output to the generator; and (3) it would easily allow a broad range of gear ratios (thus transfering various loads) to be analyzed in different sea conditions.

Figure 4.8: The chain and gear linkage system

In designing this bicycle chain and gear system both derailers were intended to be used to quickly switch gears and maintain tension. As the turbine output caused the chain to rotate in a counter-clockwise direction (which is opposite the direction of rotation on a bicycle) the free-

wheel (rear) derailer was found to be useless. Its tension arm worked in the wrong direction to keep the chain in tension or to shift gears. The next best way to change gears and maintain chain tension was to attach the freewheel and generator assembly to the backing board via two long slots and four nuts and bolts to fix it in place manually anywhere along those slots. The generator was directly linked to the freewheel in a rigid assembly. Generator load (and thus output power) would increase with its rpm, which would tend to slow down the turbine. A proper gear ratio would impendance match the system for a given sea condition to transfer the greatest rpm to the generator to produce the maximum power.

D. Internal Torque of the System

Despite all attempts to eliminate the internal torque of the system as a whole, there was a noticeable resistance to motion exhibited by the system while undergoing testing in the 380 foot wave tank. The starting torque of the system was determined by attaching a small weight spring scale to the turbine output bicycle gear at a set distance (3.5 inches) from the center of the output shaft and measuring the amount of force necessary to put the turbine into motion. The internal (starting) torque is thus defined by the same relationship as eq. 4.1

$$T = Fd \qquad 4.4$$

The internal torque of the turbine assembly alone was measured with the chain unattached to the turbine bicycle gear, and then the total torque at each one of the gear ratios was measured (see Fig. 4.9 below, and Appendix VI).

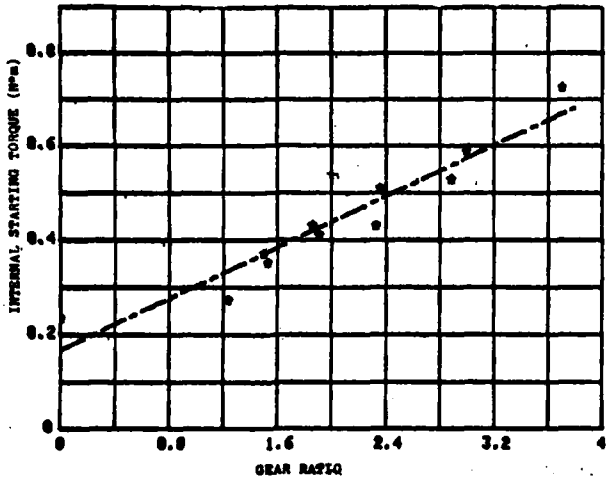

Figure 4.9: Internal starting torques of the system.

The table is useful in examining the mechanical properties of the system. The internal torque of the turbine alone of .24 N*m represents the internal friction of the system. That is a fixed inefficiency whose relative impact decreases as the actual generator load increases to impendance match the system in greater sea conditions. The starting torque of the system increases in a roughly linear relationship with the gear ratio, which is to say that as the gear ratio was increased a certain generator rpm would place a greater load upon the system. Part of this internal friction was quite noticeable. The moving rotor blades and disks scraped against each other during each rotation. Once the turbine was set in motion the torque required to keep it in motion decreased. This reduced driving torque was not however, measured.

V. ANALYSIS OF THE COMPLETED PNEUMATIC WAVE ENERGY DEVICE

A. The Capture Chamber

The capture chamber remaining from the work of Trop and Casey (1980) was used for the pneumatic wave energy conversion system investigated in this study. A critical aspect of optimizing the performance of the system was matching the frequency of the internal water column oscillations with the incident seawaves. Before performing any analysis on the capture chamber in the water, the author decided that the air flow through the system could be made less turbulent by fiberglassing the interior of the chamber into a smoother aerodynamic form. By the end of October the capture chamber was ready for extensive analysis in the 380 foot wave tank (see Appendix VII).

The frequency of the internal water column oscillations is defined by equation 3.9

$$fc = \frac{1}{2\pi}\sqrt{\frac{g}{ls + ls'}} \qquad 5.1$$

which shows the dependence of that frequency upon the submerged length and the added "effective" length. By running a series of waves at different frequencies past the capture chamber at a fixed submergence length it was possible to determine the water column frequency. The internal water column frequency would be the same as the incident wave frequency at the point of maximum amplification of the incident wave within the capture chamber, which would occur 90 degrees out of phase with the incident wave (Kinsler and

Frey, 1962). To observe the phase relationships of the incident waves and the internal water column a plexiglass window was placed in the side of the capture chamber. The wave and water column heights were measured by the use of sonic guages. The capture chamber was analyzed at two different submergences (12" and 18") with an unobstructed nozzle entrance/exit and with a series of wooden disks with various size holes in the center of each fixed over the nozzle to simulate the possible damping effects of the turbine (see Fig. 5.1 and Appendix VIII).

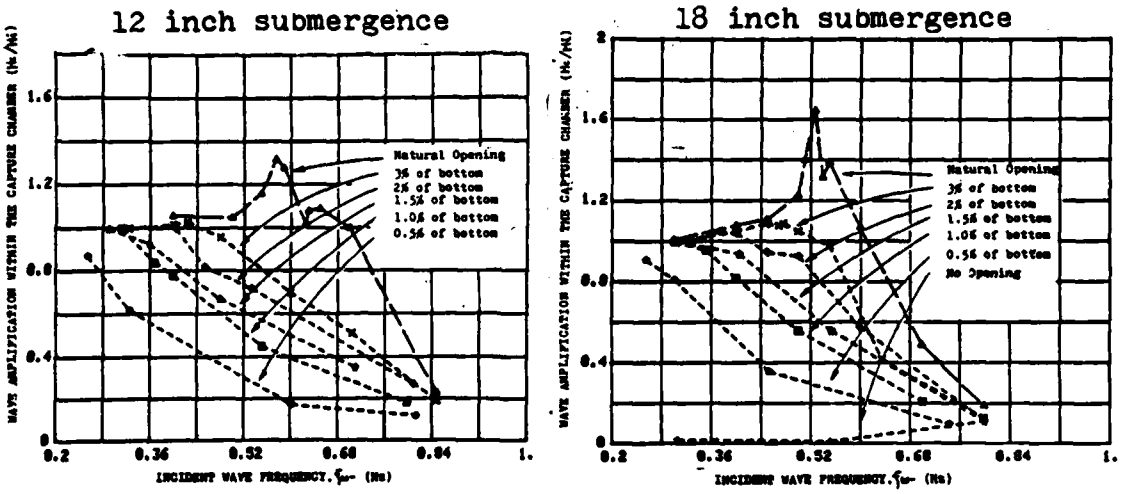

Figure 5.1: Amplification curves of the capture chamber.

From these curves it was simple to determine what submergence depth was necessary to match the internal frequency with that of the incident waves. For this capture chamber it was found that a submergence of 12 inches matched the frequencies at .575 Hz. Non-dimensionalized terms are important for possible future applications. The

non-dimensionalized submergence is defined by

$$\frac{\ell s}{D} \qquad 5.2$$

and the non-dimensionalized frequency is defined by

$$2\pi f \sqrt{\frac{D}{g}} \qquad 5.3$$

Thus, a submergence of .42 of the diameter would match the frequencies at 1.105, and a submergence of .28 of the diameter would match the frequencies at 1.199.

From this data it is also possible to verify the theoretical expression for the added-mass, which for a circular water column is

$$a(w) = \rho \frac{D^3}{3} \left[1 - \frac{(KD)^2}{15} + \frac{(KD)^4}{525} - \ldots \right] \qquad 5.4$$

where K is the wave number defined by

$$K = \frac{2\pi}{\lambda} \qquad 5.5$$

The actual added-mass is directly related to the "effective" added length, determined from equation 5.1, according to the relationship

$$a = \rho \text{ volume} = \rho \frac{\ell s \, \pi D^2}{4} \qquad 5.6$$

where $\frac{\pi D^2}{4}$ is the cross-sectional area of the water column. Table 5.1 displays the agreement between the theoretical and experimental results. The deviation is doubtlessly due to the neglect of air compressibility factors.

Submergence	Frequency	$\ell s'$	Added-mass		Deviation
			Experimental	Theoretical	
12 inches	.575 Hz	1.47 Ft.	28.05 slugs	26.1 slugs	7%
18 inches	.530 Hz	1.46 Ft.	27.87 slugs	26.1 slugs	7%

Table 5.1: Theoretical and actual added-masses.

The final analysis of the capture chamber, prior to the completed system testing, was conducted to determine the actual range of damping which the turbine could impose upon the air flow. This was done at both submergence depths (12 inches and 18 inches) by securing the turbine on top of the capture chamber in the wave tank; the generator was not linked to the turbine. A similar series of waves at different frequencies as was run past the capture chamber alone was run past the chamber and turbine assembly with the turbine fixed and not moving and then with the turbine allowed to spin freely.

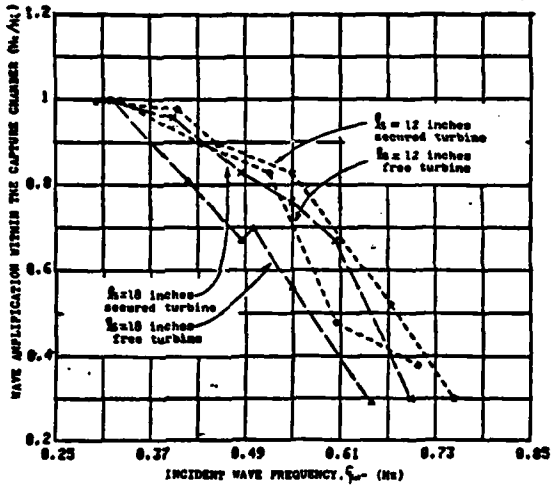

Figure 5.2: Amplification curves of turbine damping.

It is important to observe that the turbine damping curves produced (see Fig. 5.2) conform nicely to the shape of the curves previously developed for the chamber alone with a damped opening of 1.0 to 1.5% (see Fig. 5.1). As expected, the freely spinning turbine obstructs the air flow more than the fixed turbine and thus shows less amplification.

B. Pneumatic Device Analysis in a Monochromatic Sea

With the turbine and generator assembly secured to the top of the capture chamber the completed pneumatic wave energy conversion device was an impressive sight rising some 4 meters out of the water in the 380 foot wave tank. A rubber gasket between the turbine and generator assembly and the top of the capture chamber sealed the connection to prevent any air leaks. The pneumatic device was towed to the end of the tank near the wave generating board to reduce the possible effects of reflection from the far "beach" of the tank. As shown in Figure 5.3 below the pneumatic device was finally ready for its "at-sea" trials.

Figure 5.3: Pneumatic wave energy conversion device in the 380 foot wave tank

The over-riding purpose behind this analysis was to optimize the actual delivered power. To this end the procedure for the wave tank testing was to first match the frequency of the internal water column oscillations with that of the incident wave. Common wind generated sea waves have frequencies that range from .01 to 10 Hz. For an incident wave of .530 Hz., the capture chamber was submerged to a depth of 18 inches to match the frequencies. By adjusting the stroke of the wave generating board (by using different span settings), waves of different heights could be created. The pneumatic device's generator was connected in series with the strip chart recorder. Two channels of the recorder were used to measure the sinusoidaly varying incident wave height and voltage produced by the turbine. The delivered power, as explained in equation 4.3 is

$$P = \frac{V^2}{R} \qquad 5.7$$

where R=7 ohms.

A typical strip chart recording and the author's original notation's upon it is presented in Appendix IX. As the wave probe was located several meters ahead of the capture chamber, the wave heights recorded at the probe were not necessarily those of the wave as it passed the capture chamber at that moment. The window in the side of the capture chamber allowed one to note that the phase lag between the water column motions and the incident wave profile. This phase lag

appeared to be very close to 90 degrees (see Appendix X), which indicates that the device was indeed in resonance. The turbine reached its operating rotation rate (as noted by the voltage output) fairly rapidly and then settled down to a small sinusoidal variation in speed as it slowed down each time the air flow switched directions. The loaded system had a run down time of less than 5 seconds.

An important factor in the optimization of the pneumatic device is its antenna focusing and the effect of a row of such devices. The walls of the wave tank reflect the radiations of the pneumatic device creating the effect of identical pneumatic devices located beyond the wall, as illustrated in Figure 5.4 below. The boundary of the tank wall can be seen as the mid-point between the pairs of pneumatic devices. Thus the "devices" are located approximately 25 feet apart (7.62 meters). As this separation distance is greater than the allowable separation of 2.8 m for a .530 Hz wave (as explained in equation 2.15) the pneumatic device acts as a single point source. This means it is operating at its most efficient level as an antenna.

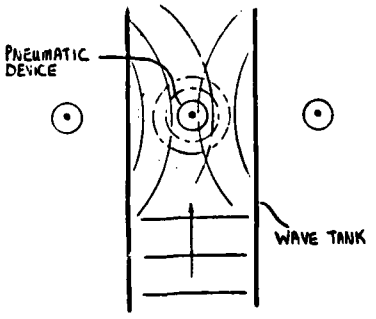

Figure 5.4: Antenna focusing within the 380 foot wave tank.

In the first series of fully operational tests a minimal wave height of 6.8 inches was generated at .530 Hz. Different gear ratios were tested at that incident wave in separate runs (see Appendix XI). This was done to determine which gear ratio transferred the proper amount of load from the generator to the turbine for maximum power production. The results (see Fig. 5.5) show that a gear ratio of 42 to 28 (1.50) produced the power, and is consequently the most efficient gear ratio for that wave.

For the next series of testing it was decided to keep the gear ratio constant at the just discovered optimum ratio of 1.50 and measure how well the system would work in a monochromatic sea at .530 Hz. but with ever increasing incident wave heights. This would represent a sea which had developed more either through a stronger wind, greater duration of the wind, or greater fetch (effective distance over which the wind acts). The results (see Fig. 5.6) show that the power increases steadily, but the efficiency reaches a maximum of 12.9% and gradually begins to decrease as the incident wave height increases. This is easily understood for the incident wave power increases with the square of the incident wave height (as explained in eq. 2.5).

The author next decided to develop several performance curves of efficiency vs. gear ratio at several incident wave heights to observe whether or not the 1.50 ratio would always be the ideal. All 10 gear ratios were analyzed against

incident waves of 8 and 10 inches. The results (combined in Figure 5.5) reveal that the system becomes more efficient in incident waves of greater height, and the location of maximum efficiency on the curves shifts to the greater gear ratios with the greater incident waves.

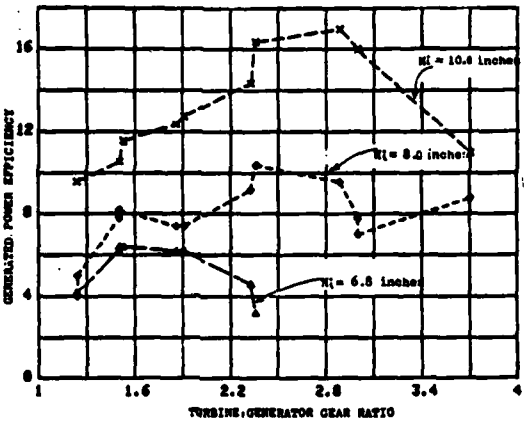

Figure 5.5: Efficiency vs. gear ratio at various incident wave heights.

The optimum gear ratio for an incident .530 Hz. wave of 6.8 inches was 1.5, at 8 inches it was 2.36, and at 10 inches it had increased to 2.89.

As the gear ratio of 52 to 18 (2.89) had proven to be the most efficient in a greater sea than 1.50, it was decided to see just how well it would function in waves varying from less than 5 inches to greater than 14 inches. As anticipated, at the lower incident wave height range it was a little less efficient than the 1.50 gear ratio, but in greater waves it proved itself to be ideal. A power output of 86.5 watts was attained, for an efficiency of 35.6%. Of more interest, perhaps, is that the resulting performance curves (combined with those of the 1.50 gear ratio in

Figure 5.6 below) show that the 2.89 gear ratio had not necessarily reached their maximum efficiency at 35.6%.

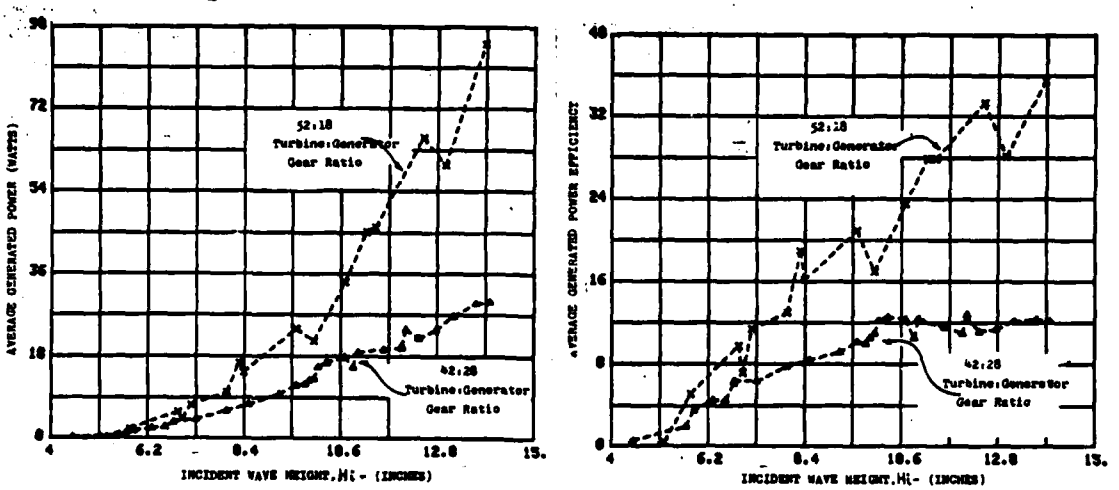

Figure 5.6: Power and efficiency performance curves for the pneumatic wave energy conversion device in a .530 Hz. monochromatic sea at 1.5 and 2.89 gear ratios.

Further wave heights were not run at the 2.89 gear ratio because the platform securing the capture chamber during the high wave testing started to shake excessively.

C. Pneumatic Device Analysis in a Random Sea

After the data from the monochromatic sea testing had been gathered and analyzed it was decided to go back into the 380 foot wave tank and investigate its performance in a random sea. Although by that point the tank time had been almost completely scheduled, three days of tank time were squeezed in. Initially the author wanted to evaluate the device in a random sea defined by the Pierson-Moskowitz energy spectrum for a fully developed sea. Mechanical difficulties with the computer precluded the use of a Pierson-Moskowitz wave. Instead, a computer generated irregular

wave was constructed by specifying its spectral form in a controllable frequency domain. Mechanical problems with the tank's beach limited the maximum amplitude of the generated waves. A resistance wire gauge was placed just forward of the device in the wave tank and its readings were fed into the control room computer, which recorded and analyzed the irregular wave. At the same time the voltage produced by the generator was fed into the strip chart recorder, in series with a 7 ohm resistor as before.

The first recorded irregular wave had a significant wave height, Hs. of 6.5 inches, defined as the average of the highest third waves. The irregular wave (see Appendix XIII) caused the turbine to rotate in fits and spurts, but did not produce a steady output. As the wave was repeated in 42 second intervals, so to was the voltage output recorded on the strip chart. The average developed voltage was calculated by adding up the areas beneath the voltage "peaks" and dividing by the amount of time covered. The incident wave power was calculated according to eq. 2.5

$$P = \frac{\rho g H^2 C g b}{8} \qquad 5.8$$

where H is the average of the highest third waves, Hs. Thus, for irregular run no. 1 the incident wave power was 54 watts. The calculated average voltage was .74 v which represented a developed power of .08 watts, for an efficiency of .1%. The comparable device efficiency for a monochromatic sea of 6.5 inches was 4.5%. Thus this represents a signifi-

cant decrease in efficiency.

Another irregular wave was generated with a significant wave height of 9.5 inches. The calculated average voltage was 2.1 v which represented a developed power of .64 watts (see Appendix XII), for an efficiency of .6%. The comparable device efficiency for a monochromatic sea of 9.5 inches was 10%. Although this still represents a significant decrease in efficiency it is much less of a decrease than in the first irregular wave run. This indicated that the efficiency could indeed be improved in a random sea.

Observations of the device in the random sea revealed that the internal water column oscillations were not rhythmic, and that the turbine again failed to maintain some rotations at all times, even with the greater incident wave. One of the solutions to the later problem was then briefly investigated. A flywheel would smooth out the response of the turbine to the incident waves and thus prevent it from having to overcome its initial starting torque once every two or three seconds. A flywheel was added to the device by securing a set of metal washers to the turbine output gears. All the washers together weighed 1.30 lbs. They were split into five roughly even groups and placed along the five radial arms of the larger gear at a distance of 2.2 inches from the center of the output shaft. The same irregular wave as shown in Appendix XII (with a significant waveheight of 9.5 inches) was again run past the pneumatic device. The

flywheel had a slight, but noticeable, effect. The peaks of the voltage output were reduced by at most .1 volts, and the duration of the peaks was extended perhaps .2 seconds in some cases. Although this produced no overall change in performance, it does indicate that a flywheel could be used to smooth out the performance of the system. The flywheel the author quickly added on had minimal effect simply because it did not increase the mass moment of inertia enough.

VI. CONCLUSIONS AND DISCUSSION

This study has verified that the performance of a pneumatic ocean wave energy conversion device can indeed be optimized. The internal water column oscillations obey the equation of motion. By varying the length of submergence the internal frequency can be controlled to match the frequency of the incident waves. This resonant condition both strengthens the amplification of the incident wave within the capture chamber and produces antenna focusing of the incident wave front towards the device. The use of a chain-gear system allows the generator load to be varied to achieve impedance matching with the pneumatic device for a given incident wave. As the incident wave power increases the most effective turbine:generator gear ratio becomes greater and the efficiency increases.

During monochromatic wave testing a maximum efficiency of 35.6% was achieved. Efficiencies dropped off rapidly in wave conditions of less incident power. This indicates that a significant internal friction exists, whose effect is relatively constant and thus has less impact on waves of greater incident power. The swift run down time for the pneumatic device of less than 5 seconds reflects the serious effect of the internal friction. Efficiencies over the entire range of incident wave powers would be improved by reducing this steady internal friction. A prototype of this pneumatic device, four times greater in scale, has been built

and is currently located in San Diego for research. With run down times of 8 minutes unloaded and 4 minutes loaded, the prototype promises minimal internal friction and improved performance.

During random sea testing in the 380 foot wave tank the system efficiency was greatly reduced. There are two significant reasons for this. First, the majority of the wave heights were on the minimal side which, due to the pneumatic device's internal friction, were inherently less efficient in this study. Secondly, as the frequencies shifted and the incident wave heights varied, the resonance of the internal water column was interfered with and the turbine had to continually overcome the greater internal starting torques.

Although this study was successful in proving that a pneumatic ocean wave energy conversion device's performance can be optimized, of equal interest is the guidance it gives for directing further research to prepare the system for commercial applications. The following topics are presented for further study:

(1)Air Compressibility Effects - By developing a mechanism to vary the air cavity within the capture chamber, air compressibility can be used to control water column motions. In this manner the frequency of internal water column oscillations can be made to resonate with the incident waves, as shown in equation 3.8.

(2) Air Flow - A study of the air flow within the device would indicate where further modifications could be performed to make the flow more aerodynamic. To this end, the prototype has moveable outer vanes to smoothly direct the air flow into the spinning rotors regardless of the air flow velocity.

(3) Generator:Turbine Linkage - A simple improvement on the design developed in this study would be the replacement of the bicycle gear system with a nylon cord system. Such a linkage would cause less friction and allow for an uninterrupted range of turbine:gear ratios.

An additional possibility here would be to have the rotating turbine output shaft actually be the internal shaft of a magnetic generator. Such a system might offer the least amount of resistance.

(4) Flywheel - The use of a flywheel in any further applications of the device would be a simple and effective improvement. In random seas it would keep the turbine rotating and thus prevent the loss of energy in constantly having to restart the turbine from a standstill. A flywheel would also smooth out the developed power response to the incident waves. A flywheel would, ideally, slightly over-damp the response of the turbine.

(5) Active Control System - The efficiency of the system is fairly delicate and requires continual impedance matching and resonance for optimum performance. When the

device actually experiences random ocean waves it will require an active control system to maintain that optimum performance. Further analysis can define the system "settings" needed for the numerous random sea conditions to be experienced, and this data can be stored and recalled by the control system as it monitors the incident sea. Feedback control could be used for slight adjustments to maintain resonance and impedance devices in a row may only need to have a monitoring capability every 20 to 50 devices.

(6) Mooring - The mooring of this pneumatic device is a vital aspect of the system not analyzed in this study. The lens needs to be examined. For initial offshore use and analysis the pneumatic devices could be secured to oil rigs.

From ~~this~~ The research it is clear that pneumatic wave energy conversion is a promising concept. ~~Imagine~~ With several hundred of these devices situated some 100 km off the coast of the Pacific Northwest. ~~The devices would be~~ moored to the bottom in positions taking advantage of natural seamounts in the area to focus waves towards themselves. Each device would be producing from 50 to 200 kW which would be transferred back to shore via long power lines along the bottom. Such a vision is within the foreseeable future.

LIST OF REFERENCES

Budal, K., and J. Falnes, "Proposals for Conversion of the Energy in Ocean Waves," Institute for eksperimental fysikk. Norges Tekniske hogskole, Trondheim, Internal Report, 1974.

Falnes, Johannes and Kjell Budal, "Wave Power Conversion by Point Absorbers," Norwegian Maritime Research, (Vol. 6. No. 4, 1978), pp.2-11.

Jolly, P.C. and J. Newmaster, "The Pneumatic Turbine," (Unpublished Paper) U.S. Naval Academy, 1979.

Kinsler, Lawrence and Austin Frey, Fundamentals of Acoustics. New York: John Wiley and Sons, 1962.

McCormick, Michael E., "An Analysis of Optimal Wave Energy Conversion by Two Single-Degree-of-Freedom Devices," Journal of the Waterway, Port, Coastal and Ocean Division, American Society of Civil Engineers (In Review), 1981.

_____. Ocean Wave Energy Conversion. New York: John Wiley and Sons, 1981.

_____. Ocean Engineering Wave Mechanics. New York: John Wiley and Sons, 1973.

_____. "Wave Energy Conversion in a Random Sea." Proceedings of the 13th Intersociety Energy Conversion Conference, Warrendale, Pa.: Society of Automotive Engineers, 1978, pp. 2186-2193.

McCormick, Michael and Eugene Burcher, "Pneumatic Wave Energy Conversion," submitted to the First US-China Conference on Energy Resources and Environment, Peking (PRC) 1982.

Trop, Byron and Thomas Casey, "Improvement and Analysis of a Pneumatic Wave Energy Converter," (Unpublished Paper) U.S. Naval Academy, 1980.

APPENDIX I: Computer Program for Wind Tunnel Analysis

```
4 GO TO 100
6 CLOSE
9 PRINT "<<<<<<<<<< END OF PROGRAM >>>>>>>>>>"
10 END
25 STOP
36 PRINT @9:"C"
37 PRINT @9:0,2
38 END
40 PRINT @9:"C"
41 PRINT @9:0,3
42 END
100 REM*************************************************************************
110 REM PNEUMATIC WAVE ENERGY CONVERSION DEVICE TURBINE ANALYSIS
120 REM          DATE:  4 SEPTEMBER, 1981
130 REM  BASED ON FILE 11 IN USNA AEROSPACE "WIND TUNNEL" TAPE
140 REM
150 REM   USER DEFINABLE KEYS:  TO USE STEP SCANNER MANUALY
160 REM                        9=TORQUE
170 REM                       10=RPM
180 REM
190 REM                          REWRITTEN BY S.SURKO'82, USNA
200 REM                           LAST REVISION AND CALIBRATION DONE ON
210 REM                           1 OCTOBER, 1981
220 REM*************************************************************************
230 INIT
240 M=1
250 DIM H(3),R(10),K(3),V(10)
260 A$="N"
270 R=0
280 SET KEY
290 S2=1
300 PAGE
310 K(2)=0
320 K(3)=0
330 PRINT "DATE";
340 INPUT D$
350 PRINT "CONFIGURATION ";
360 INPUT C$
370 F1=0
380 PAGE
390 M1=0
400 PRINT "_____________________________________________________"
410 FOR I=1 TO 600
420 NEXT I
430 H(2)=0
440 H(3)=0
450 PRINT "RUN NO.";M
460 PRINT "WHEN READY TYPE `IEST`"
470 INPUT Z$
480 REM***** CLEAR SCANNER (HP 3495A) *****
490 PRINT @9:"C"
500 FOR Q=1 TO 5
510 FOR I=2 TO 3
520 PRINT @9:0,I
530 REM***** PROCEEDING TO TAKE A VOLTAGE READING *****
540 GOSUB 650
550 V(I)=N
560 FOR J=1 TO 50
570 NEXT J
580 H(I)=H(I)+V(I)
```

```
590 NEXT I
600 NEXT Q
610 FOR T=1 TO 20
620 NEXT T
630 GO TO 750
640 REM*** SUBROUTINE TO CAUSE 3495A TO ACQUIRE A VOLTAGE SAMPLE ***
650 WBYTE @63,95:
660 WBYTE @36:
670 WBYTE @36:66,59,67,61,62
680 WBYTE @63,95:
690 PRINT @4:"T3"
700 INPUT @4,32:B$
710 WBYTE @63,95:
720 N=VAL(B$)
730 RETURN
740 END
750 REM
760 REM*** 24 SEPT. REVISION-AVERAGING ROUTINE ***
770 V(2)=H(2)/5
780 V(3)=H(3)/5
790 PRINT "DATE ";D$
800 REM*** THE FOLLOWING ARE LINEAR CALIBRATION CONSTANTS ***
810 F2=166.8
820 F3=-168.8
830 REM***COMPUTATION AND DISPLAY ***
840 W=0.00504*F1
850 PRINT USING 860:"AIR SPEED",W,"M/S"
860 IMAGE 9A,21X,3D.3D,2X,3A
870 T=(V(2)-K(2))*F2
880 PRINT USING 890:"TORQUE",T,"N*M"
890 IMAGE 6A,24X,3D.3D,2X,3A
900 S=(V(3)-K(3))*F3
910 PRINT USING 920:"RPM",S,"RPM"
920 IMAGE 3A,27X,3D.3D,2X,3A
930 REM*** NOW CALCULATE THE POWER ***
940 P=T*S*2*3.141593/60
950 PRINT USING 960:"POWER",P,"N*M/S"
960 IMAGE 5A,25X,3D.3D,2X,5A
970 M=M+1
980 M1=M1+1
990 IF M=2 THEN 1000
1000 PRI "-----------------------------------------------------------"
1010 IF M1=3 THEN 1030
1020 GO TO 410
1030 PRINT
1040 COPY
1050 PAGE
1060 GO TO 390
1070 REM*** 3 SEPT. REVISION-ACCOUNTING FOR TEAR READINGS ***
1080 K(2)=V(2)
1090 K(3)=V(3)
1100 PRINT C$
1110 PRINT "THIS FIRST RUN HAS BEEN A TEAR RUN TO ZERO THE INSTRUMENTS"
1120 REM** CHECK:WITH NO NEW INPUTS, RUN NO.2 VALUES SHOULD EQUAL 0 **
1130 PRI "-----------------------------------------------------------"
1140 PRINT "INPUT TEST VELOCITY THROUGH TURBINE (F/M)";
1150 INPUT F1
1160 GO TO 410
```

APPENDIX II: Typical Computer Program Printout

```
RUN NO.1
WHEN READY TYPE 'TEST'

DATE 15 JANUARY, 1982
AIR SPEED                          1.888  M/S
TORQUE                            -0.034  N*M
RPM                                0.881  RPM
POWER                              0.000  N*M/S
VERTICAL
THIS FIRST RUN HAS BEEN A TEMP RUN TO ZERO THE INSTRUMENTS

INPUT TEST VELOCITY THROUGH TURBINE IF NEED
RUN NO.2
WHEN READY TYPE 'TEST'

DATE 15 JANUARY, 1982
AIR SPEED                          2.747  M/S
TORQUE                            -0.001  N*M
RPM                              507.370  RPM
POWER                             -0.067  N*M/S

RUN NO.3
WHEN READY TYPE 'TEST'

DATE 15 JANUARY, 1982
AIR SPEED                          2.747  M/S
TORQUE                             0.127  N*M
RPM                              435.909  RPM
POWER                              5.811  N*M/S
```

APPENDIX III: Phase One and Two Turbine Wind Tunnel Test Results

TURBINE WIND TUNNEL TESTS

DATE	RUN	STAND-STILL VELOCITY(M/S)	ACTUAL VELOCITY(M/S)	TORQUE (N·M)	RPM	POWER (WATTS)
6 OCT81	1	1.56	———	0.01	174	0.13
"	2	1.56	———	0.002	177	0.04
"	3	1.56	———	0.02	169	0.37
"	4	1.56	———	0.04	158	0.66
"	5	1.56	———	0.05	153	0.76
"	6	1.56	———	0.08	137	1.08
"	7	1.56	———	0.11	114	1.34
"	8	1.56	———	0.11	106	1.23
"	9	1.56	———	0.13	85	1.11
"	10	1.56	———	0.15	39	0.62
"	11	1.56	———	0.16	0	0
6 OCT81	1	1.92	1.92	0.66	0	0
"	2	1.92	1.84	0.52	19	1.03
"	3	1.92	1.74	0.45	40	1.86
"	4	1.92	1.67	0.39	58	2.38
"	5	1.92	1.63	0.35	73	2.63
"	6	1.92	1.57	0.29	93	2.82
"	7	1.92	1.53	0.27	99	2.74
"	8	1.92	1.43	0.17	137	2.50
"	9	1.92	1.40	0.13	152	2.03
"	10	1.92	1.29	0.05	192	1.08
"	11	1.92	1.26	0.02	218	0.46
7 OCT81	1	2.23	———	0.02	285	0.69
"	2	2.23	———	0.05	269	1.45
"	3	2.23	———	0.11	239	2.76
"	4	2.23	———	0.17	209	3.75
"	5	2.23	———	0.25	181	4.69
"	6	2.23	———	0.31	150	4.82
"	7	2.23	———	0.33	137	4.77

8	2.23	———	Ø.36
9	2.23	———	Ø.42
1Ø	2.23	———	Ø.51
11	2.23	———	Ø.57
12	2.23	———	Ø.61
13	2.23	———	Ø.68
1	1.18	———	Ø.Ø
2	1.18	———	Ø.ØØ4
3	1.18	———	Ø.Ø35
4	1.18	———	Ø.125
5	1.18	———	Ø.21
6	1.18	———	Ø.296
7	1.18	———	Ø.435
8	1.18	———	Ø.4Ø4
1	2.75	———	Ø.Ø
2	2.75	———	Ø.13
3	2.75	———	Ø.24
4	2.75	———	Ø.32
5	2.75	———	Ø.46
6	2.75	———	Ø.61
7	2.75	———	Ø.99
8	THE GEARS	SLIPPED	AT GREATER

APPENDIX IV: Damping Effect of Turbine Revolutions

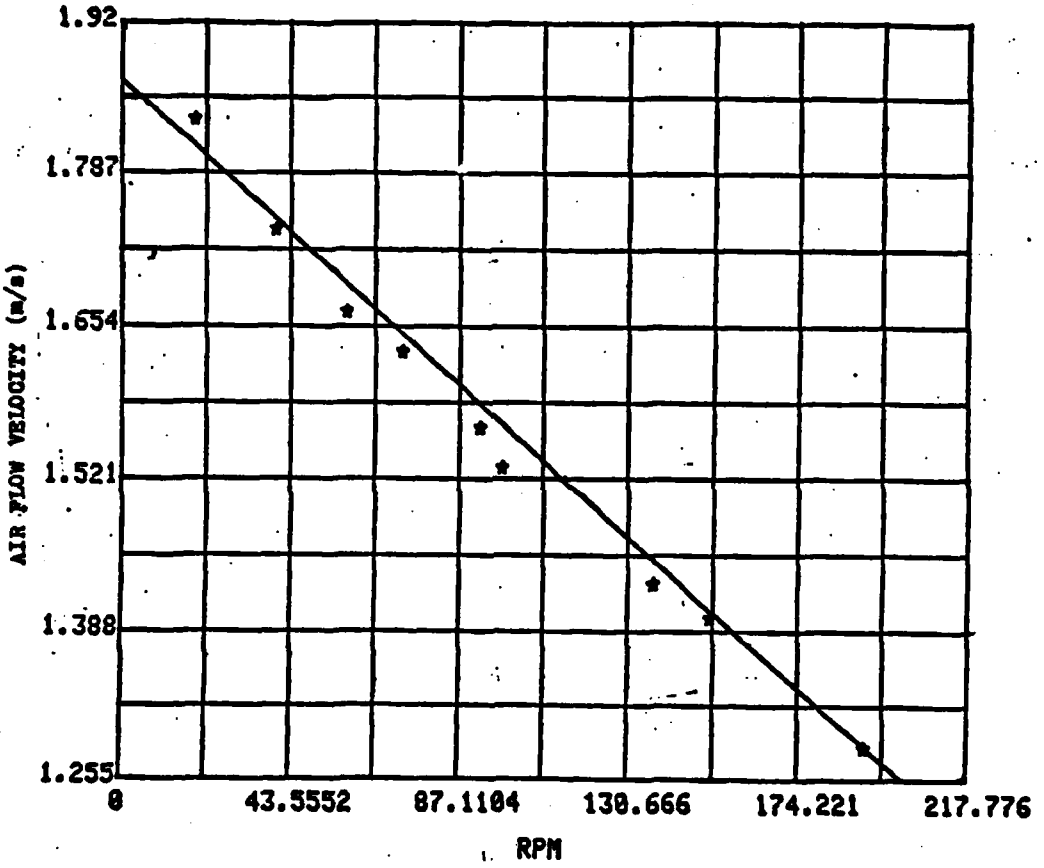

1. TC25G GENERATOR CHARACTERISTICS

1.1 DESCRIPTION

The TC25G generator is a high-efficiency permanent-magnet dc generator, designed particularly for low-rpm renewable energy applications such as charging 12-volt batteries.

The stator is a two-pole ceramic magnet assembly, power-saturated after construction to avoid particle adhesion. The magnetic circuit of the stator is completed via the heavy-duty drawn steel case.

The armature is a ten-slot double-series-wound type. Current is delivered through two long-life carbon brushes, sealed inside the case. The 5/16 inch armature shaft runs in prelubricated bronze bushings.

1.2 DIRECTION OF ROTATION

The stator magnets are positioned for maximum output when the generator shaft rotates in a clockwise direction as viewed from the shaft end of the case.

While no damage is done by reverse rotation, the output is reduced and the polarity is reversed.

1.3 USE AS A MOTOR

The TC25G generator can be used as a motor when required - for instance to start a Darrieus rotor, or as a motor-generator for a bicycle. Generally the motor driving voltage for equivalent torque would be higher than the generator output at the same rpm.

In cases where the TC25G is used as a motor-generator, the battery-charging system can be designed for isolated charging of several series-connected batteries. Please contact Thermax for engineering advice for unusual applications.

1.4 MULTIPLE GENERATORS

Several TC25G generators can be used in tandem to generate higher voltages or currents than from a single unit.

All tandem generators must rotate as closely as possible at the same speed. They may be connected in series for higher voltage, in parallel for higher voltage and current. Connection rules for polarity are the same as for batteries.

TC25G GENERATOR

2. MECHANICAL SPECIFICATIONS

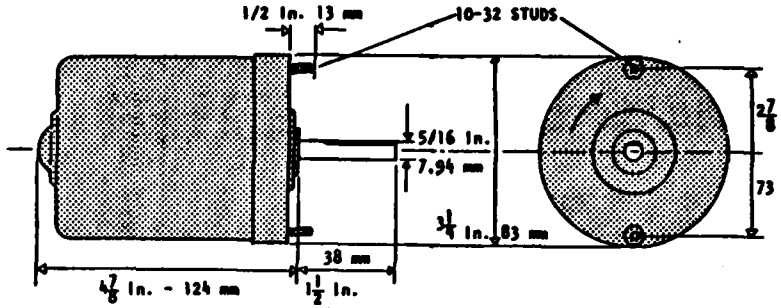

WEIGHT 3.5 lb. 1.6 kg.

3. ELECTRICAL SPECIFICATIONS

3.1 The TC25G generator can be used for small power production over a range of voltages. The most common voltage used is 12 volts; for charging a 12-volt battery 13,5 volts is used.

3.2 RATINGS

Rated power 25 watts	-	Peak power 150 watts
Rated voltage 12 volts	-	Peak voltage 100 volts
Rated current 2 amps	-	Peak current 7 amps
Internal resistance	-	7 ohms

3.3 VOLTAGES

Voltages frequently used are:

6	(Electric fences)
9	(Some communications equipment)
12	Most common voltage for dc lights, pumps, appliances, electronic equipment.
24	(Some motors)
28	(Aircraft equipment)
32	(Marine equipment)

Generally, higher power outputs are obtained at higher voltages, since the power in watts is the product of voltage and current.

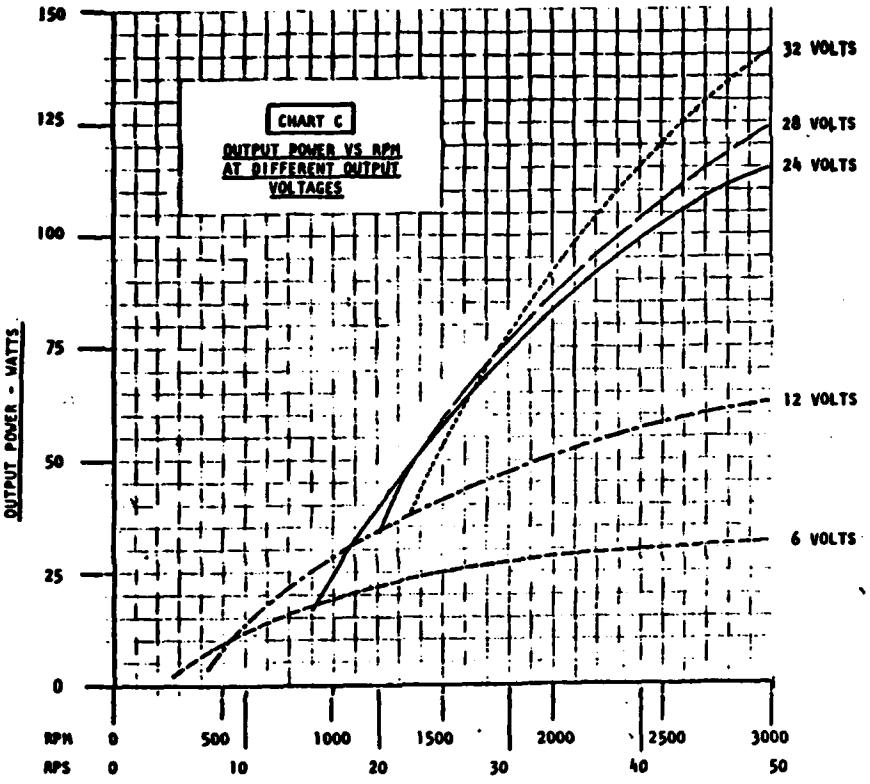

3.5 HEATING

The TC25G generator should be adequately ventilated while in operation. High current delivery causes heating in the windings, which must be allowed to dissipate.

If ventilation holes must be drilled in the case, the chips should be removed by vacuum, while drilling, to avoid adhesion of particles to the magnets.

If necessary, a small fan can be mounted on the drive shaft.

3.6 BRUSHES

It is unlikely that the oversized generator brushes will need attention. However, should the brushes ever require replacement, either return the generator to Thermax with $12.00, covering the cost of brushes, handling and shipping, or order replacement brushes for $4.00 per pair including shipping. As special equipment is required to open and close the generator case, the first procedure is recommended.

3.7 GENERATOR HORSEPOWER

To determine the equivalent horsepower rating of the TC25G generator at different wattage outputs, refer to Chart D below.

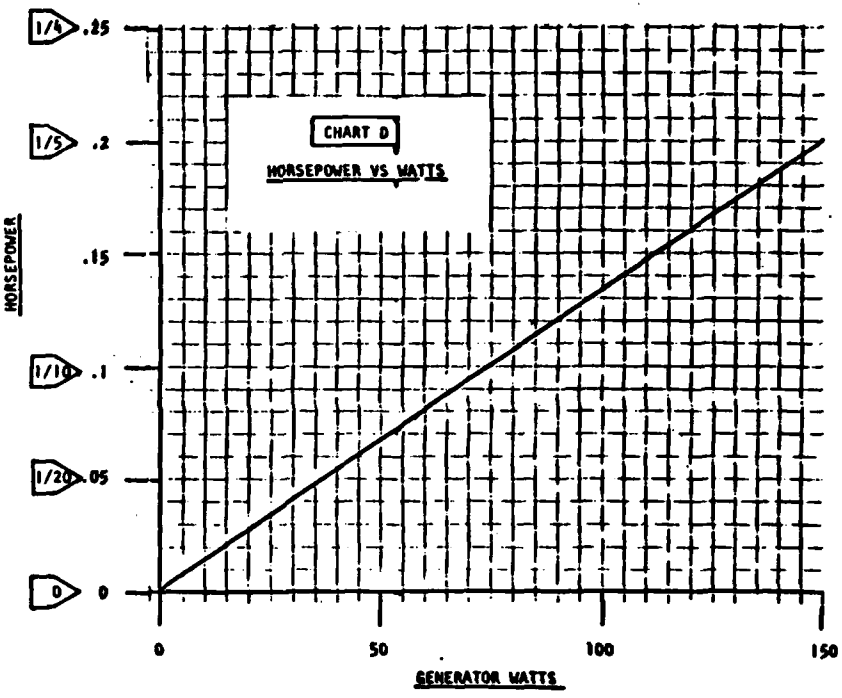

To determine horsepower at any given output voltage, output power and rpm, first obtain the wattage from Chart C, and apply that figure to Chart D to convert to horsepower.

APPENDIX VI: Internal Starting Torques of the Turbine

GEAR RATIO		FORCE (Lbf.)	DISTANCE (Feet)	STARTING TORQUE		ADDITIONAL STARTING TORQUE OF THE GEAR RATIO (N•m)
TURBINE:GENERATOR	RATIO VALUE			ft. Lbf	N•m	
TURBINE ALONE	0	0.6	.29	.174	.236	———
42:34	1.24	0.7	.29	.203	.275	.04
42:28	1.50	0.95	.29	.276	.374	.14
52:34	1.53	0.9	.29	.261	.354	.12
52:28	1.86	1.1	.29	.319	.433	.20
42:22	1.91	1.05	.29	.305	.413	.18
42:18	2.33	1.1	.29	.319	.433	.20
52:22	2.36	1.3	.29	.377	.511	.28
52:18	2.89	1.35	.29	.392	.531	.30
42:14	3.00	1.5	.29	.435	.590	.35
52:14	3.71	1.85	.29	.537	.728	.49

APPENDIX VII: 380 Foot Wave Tank Specifications

U. S. NAVAL ACADEMY HYDROMECHANICS LABORATORY — U.S.A.
ANNAPOLIS, MARYLAND 21402
TELEPHONE: (301) 267-3361

128m HIGH PERFORMANCE TOWING TANK (1979)

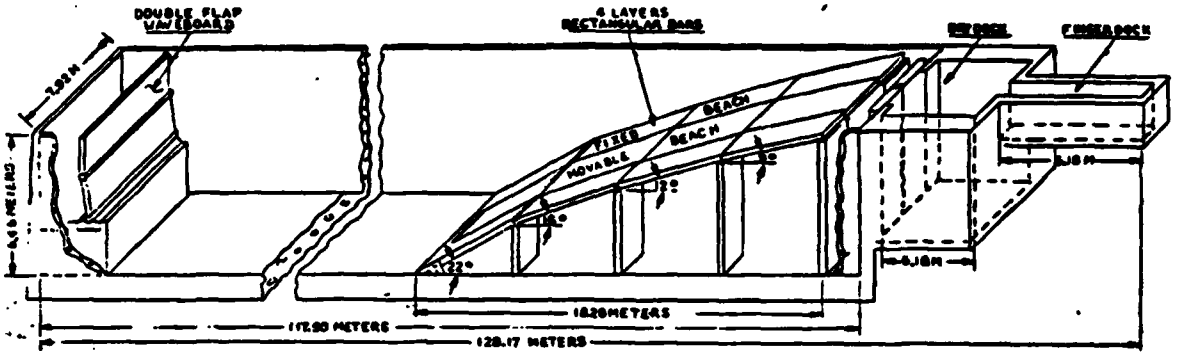

380 FOOT TANK AND WAVEMAKER

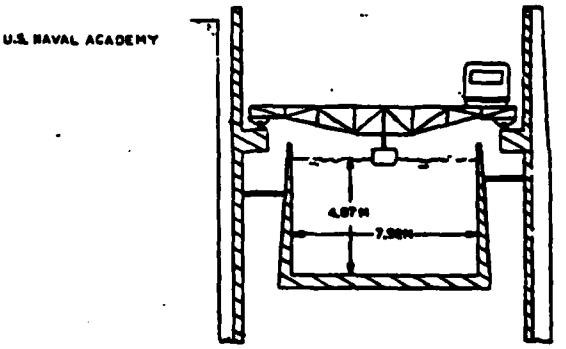

DESCRIPTION OF CARRIAGE: 1) high speed - box grider, supported on round way bearings or rulon slippers
2) low speed - supported on round way bearings (towed by high speed carriage)

TYPE OF DRIVE SYSTEM AND TOTAL POWER: twin cables attached to high speed carriage, digital control interface with computer, 2 - 150 kw D.C. motors (400% overload capability)

MAXIMUM CARRIAGE SPEED: low speed carriage - 7.6 m/s (25 fps)
high speed carriage - 14 m/s (45 fps)

OTHER CAPABILITIES: large amplitude planar motion mechanism, computer controlled testing

WAVE GENERATION CAPABILITY: regular, irregular and transient water waves, max wave 1m x 10m, wave length 0.6m - 30m

WAVEMAKER TYPE AND EXTENT: dual flap servo-hydraulic control, 7.9m x 2.7m

BEACH TYPE AND LENGTH: 4 layer of rectangular bars, 18.3m

METHOD OF IRREGULAR WAVE GENERATION: computer generated, spectral form specified in frequency domain, generated waves are analyzed and spectrum corrected until desired spectral shape is obtained.

OTHER CAPABILITIES: the "Periodic Irregular Encountered Wave Techniques for Seakeeping Test" is based on irregular wave components which are equally spaced in the encountered frequency domain. This reduces the testing time required to the reciprocal of the frequency resolution of the encountered wave harmonics

---

INSTRUMENTATIONS: PDP 11/50 in control room, PDP 11/05 for wavemaker control, laser telemetry system between carriage and shore to transmit digital data, t.v., and control channels 15 bit A/D converters on each carriage and on shore, variable reluctance force block for all force measurements, variable torque and thrust dynamometers, Hydronautics multi-T signal conditioners, planing boat and S.E.S. dynamometer, 3 axis submerged model dynamometer open water propeller dynamometers, pitot tube rakes for wake surveys, rudder torque gauges, ultrasonic and resistance wave height gauges, graphic display and/or hard copies available immediately upon completion of test run

MODEL SIZE RANGE: ship model lengths for resistance and propulsion tests 3m - 8m, for seakeeping and maneuvering testing 3m - 5m, ocean structures 1m - 2m in diameter

TESTS PERFORMED: resistance in self-propulsion in calm water and waves, seakeeping tests, open water propeller test, 3-D wake surveys, horizontal planar motion tests, various test of ocean structures, hydrodynamic forces on submerged bodies, foils, etc., capsize and dynamic stability tests, flow visualization

OTHER REMARKS: extensive software developed for standard test data base

---

PUBLISHED DESCRIPTION: proceedings of -

16th American Towing Tank Conference 1971
18th American Towing Tank Conference 1977
19th American Towing Tank Conference 1980

APPENDIX VIII: Amplification Curves of the Capture Chamber

INTERNAL WATER COLUMN OSCILLATIONS

LENGTH OF SUBMERGENCE (l_s) = 18"
WAVE FREQUENCY ~ f_w
DIMENSIONLESS FREQUENCY = $2\pi f\sqrt{D/g}$
INCIDENT WAVE HEIGHT = H_i
CHAMBER WATER COLUMN HEIGHT = H_c

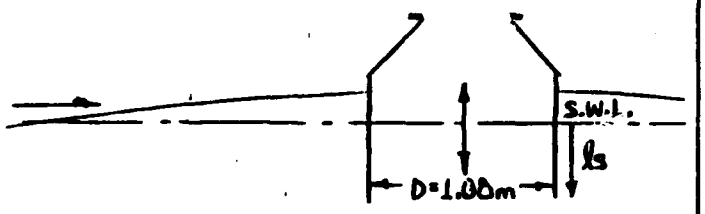

DATE	RUN	CHAMBER TOP OPENING		f_w (Hz)	DIMENSIONLESS FREQUENCY	H_i (IN.)	H_c (IN.)	H_c/H_i	OBSERVATIONS
		DIAMETER (IN.)	% OF BOTTOM						
23OCT81	1	NATURAL ~ 12.75 IN.	9	.6	1.25	3.84	4.11	1.07	
"	2	"	9	.7	1.46	2.71	1.35	0.49	
"	3	"	9	.8	1.67	4.26	.82	0.19	
"	4	"	9	.5	1.04	6.47	7.98	1.23	
"	5	"	9	.4	0.834	6.75	7.3	1.08	
"	6	"	9	.3	0.625	5.19	5.29	1.01	
"	7	"	9	.45	0.938	5.58	6.2	1.11	
"	8	"	9	.55	1.15	5.1	7.1	1.39	
27 OCT81	1	"	9	.528	1.10	5.1	8.4	1.65	
"	2	"	9	.511	1.07	5.3	7.4	1.40	
14 DEC81	34	"	9	.800	1.67	6.0	.74	.12	
"	35	"	9	.539	1.12	5.99	7.93	1.32	SONIC DROP-OUT
"	1	7/4 IN.	3	.300	0.625	3.17	3.17	1.0	
"	2	"	3	.400	0.834	5.85	6.17	1.05	
"	3	"	3	.500	1.04	6.46	6.78	1.05	
"	4	"	3	.635	1.32	8.56	3.62	0.42	
"	5	"	3	.550	1.15	6.33	6.23	0.98	

5 COPIES

INTERNAL WATER COLUMN OSCILLATIONS

LENGTH OF SUBMERGENCE (l_s) = 18"
WAVE FREQUENCY ~ f_ω
DIMENSIONLESS FREQUENCY = $2\pi f\sqrt{D/g}$
INCIDENT WAVE HEIGHT = Hi
CHAMBER WATER COLUMN HEIGHT = Hc

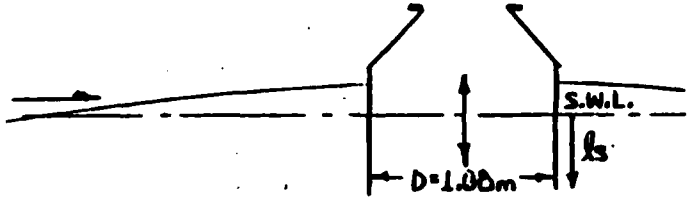

DATE	RUN	CHAMBER TOP OPENING		f_ω (Hz)	DIMENSIONLESS FREQUENCY	Hi (IN.)	Hc (IN.)	Hc/Hi	OBSERVATIONS
		DIAMETER (IN.)	% OF BOTTOM						
14 DEC81	6	7.4 IN.	3	.448	0.934	4.59	5.01	1.09	
"	7	"	3	.475	0.990	4.78	5.23	1.09	
"	8	"	3	.468	0.976	5.09	5.48	1.08	
"	33	"	3	.80	1.67	6.14	0.79	0.13	SUPERPOSITION OF REFLECTED WAVES
"	14	6. IN.	2	.304	0.634	3.15	3.15	1.00	
"	15	"	2	.401	0.836	4.49	4.62	1.04	
"	16	"	2	.501	1.04	5.10	4.75	.93	
"	17	"	2	.600	1.25	6.14	3.55	.58	
"	18	"	2	.800	1.67	5.59	0.68	.12	SUPERPOSITION OF UNSETTLED WAVES
"	19	"	2	.450	0.938	5.25	5.01	.95	
"	20	"	2	.374	0.780	4.46	4.68	1.05	
"	21	"	2	.330	0.690	4.09	4.09	1.00	
"	26	5.2 IN.	1.5	.305	0.636	3.76	3.76	1.00	
"	27	"	1.5	.405	0.844	5.14	4.85	.94	
"	28	"	1.5	.554	1.15	6.46	3.60	.56	
"	29	"	1.5	.801	1.67	5.98	0.65	.11	SUPERPOSITION OF UNSETTLED WAVES
"	9	4.25 IN.	1.0	.301	0.627	3.0	3.0	1.0	

85

4.25 IN.	1.0	.400	0.834	4.76	3.88	0.82
"	1.0	.501	1.04	5.49	3.07	.56
"	1.0	.701	1.46	6.19	1.31	.12
"	1.0	.351	0.732	3.65	3.52	.96
3.0 IN.	0.5	.301	0.627	3.46	2.81	.81
"	0.5	.454	0.947	4.78	1.70	.36
"	0.5	.744	1.55	6.17	.63	.10
"	0.5	.254	0.530	2.66	2.42	.91
TOTAL BAFFLE 0.0 IN.	0.0	.305	0.636	3.71	.06	.02
"	0.0	.551	1.15	6.46	.08	.01
"	0.0	.800	1.67	6.04	.68	.11

4 COPIES

INTERNAL WATER COLUMN OSCILLATIONS

LENGTH OF SUBMERGENCE (l_s) = 18"
WAVE FREQUENCY ~ f_w
DIMENSIONLESS FREQUENCY = $2\pi f\sqrt{D/g}$
INCIDENT WAVE HEIGHT = Hi
CHAMBER WATER COLUMN HEIGHT = Hc

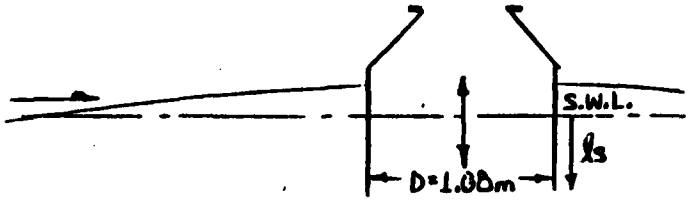

DATE	RUN	CHAMBER TOP OPENING		f_w (Hz)	DIMENSIONLESS FREQUENCY	Hi (IN.)	Hc (IN.)	Hc/Hi	OBSERVATIONS
		DIAMETER (IN.)	% OF BOTTOM						
25 JAN82	7	SECURED	TURBINE	.485	1.01	6.3	5.2	.83	AIR FLOW APX. 210 FPM
"	8	"	"	.399	.832	5.1	4.9	.96	AIR FLOW APX. 155 FPM
"	9	"	"	.314	.655	4.1	4.1	1.0	
"	10	"	"	.550	1.15	5.7	4.35	.76	AIR FLOW APX. 210 FPM
"	11	"	"	.604	1.26	4.9	3.3	.67	AIR FLOW APX. 200 FPM
"	12	"	"	.700	1.46	5.55	1.65	.30	

09

INTERNAL WATER COLUMN OSCILLATIONS

LENGTH OF SUBMERGENCE (l_s) = 12"
WAVE FREQUENCY ~ f_w
DIMENSIONLESS FREQUENCY = $2\pi f\sqrt{D/g}$
INCIDENT WAVE HEIGHT = Hi
CHAMBER WATER COLUMN HEIGHT = Hc

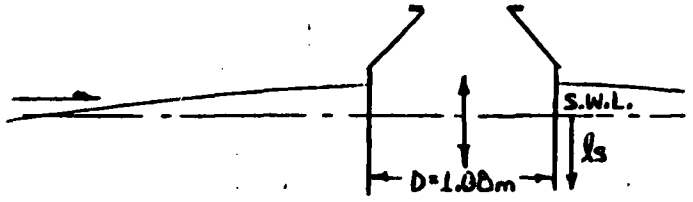

DATE	RUN	CHAMBER TOP OPENING		f_w (Hz)	DIMENSIONLESS FREQUENCY	Hi (IN.)	Hc (IN.)	Hc/Hi	OBSERVATIONS
		DIAMETER (IN.)	% OF BOTTOM						
27OCT81	3	NATURAL 12.75 IN.	9	.398	0.830	5.1	5.4	1.06	
"	4	"	9	.500	1.04	5.7	6.0	1.05	
"	5	"	9	.599	1.25	5.6	6.8	1.21	
"	6	"	9	.700	1.46	4.6	4.6	1.00	
"	7	"	9	.550	1.15	5.6	6.5	1.16	
"	8	"	9	.650	1.36	5.3	5.8	1.09	SONIC DROP-OUT
"	9	"	9	.625	1.30	5.7	5.7	1.02	
"	10	"	9	.630	1.31	5.2	5.6	1.08	
"	11	"	9	.575	1.20	5.6	7.4	1.32	
"	12	"	9	.588	1.23	5.3	6.8	1.28	
"	13	"	9	.625	1.30	5.5	5.6	1.02	
15 DEC81	8	"	9	.850	1.77	5.72	1.29	.23	SUPERPOSITION OF UNSETTLED WAVES
"	1	7.4 IN.	3	.399	0.832	5.49	5.59	1.02	
"	2	"	3	.325	0.678	3.91	3.91	1.00	
"	3	"	3	.424	0.884	5.26	5.40	1.03	
"	4	"	3	.481	1.00	5.91	5.67	.96	
"	5	"	3	.601	1.25	6.56	4.57	.70	

5 (cont'd)

INTERNAL WATER COLUMN OSCILLATIONS

LENGTH OF SUBMERGENCE (l_s) = 12"
WAVE FREQUENCY ~ f_ω
DIMENSIONLESS FREQUENCY = $2\pi f\sqrt{D/g}$
INCIDENT WAVE HEIGHT = H_i
CHAMBER WATER COLUMN HEIGHT = H_c

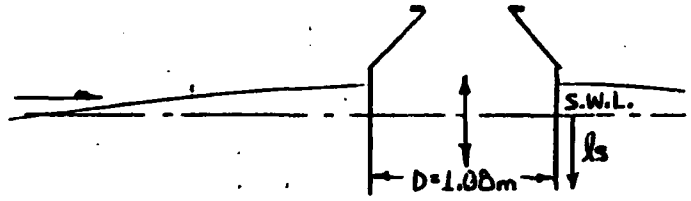

DATE	RUN	CHAMBER TOP OPENING		f_ω (Hz)	DIMENSIONLESS FREQUENCY	H_i (IN.)	H_c (IN.)	H_c/H_i	OBSERVATIONS
		DIAMETER (IN.)	% OF BOTTOM						
15 DEC81	6	7.4 IN.	3	.705	1.47	6.56	3.32	.51	
"	7	"	3	.850	1.77	5.33	1.00	.19	SUPERPOSITION OF UNSETTLED WAVES
"	9	6 IN.	2	.314	0.655	4.17	4.17	1.00	
"	10	"	2	.405	0.844	5.31	5.30	1.00	
"	11	"	2	.534	1.11	6.30	4.52	.72	
"	12	"	2	.454	0.946	5.62	4.62	.82	
"	13	"	2	.810	1.69	6.33	1.69	.27	
"	23	5.2 IN.	1.5	.290	0.605	5.07	5.07	1.00	
"	24	"	1.5	.359	0.748	5.81	5.39	.93	
"	25	"	1.5	.480	1.00	6.52	4.37	.67	
"	26	"	1.5	.711	1.48	6.88	2.43	.35	
"	14	4.25 IN.	1.0	.311	0.648	3.07	3.06	1.00	
"	15	"	1.0	.401	0.836	5.23	4.09	.78	
"	16	"	1.0	.368	0.767	5.20	4.38	.84	
"	17	"	1.0	.551	1.15	6.30	2.83	.45	
"	18	"	1.0	.799	1.67	6.0	1.07	.18	
"	19	3.0 IN.	0.5	.254	0.530	3.48	3.03	.87	

INTERNAL WATER COLUMN OSCILLATIONS

LENGTH OF SUBMERGENCE (l_s) = 12"
WAVE FREQUENCY ~ f_w
DIMENSIONLESS FREQUENCY = $2\pi f\sqrt{D/g}$
INCIDENT WAVE HEIGHT = Hi
CHAMBER WATER COLUMN HEIGHT = Hc

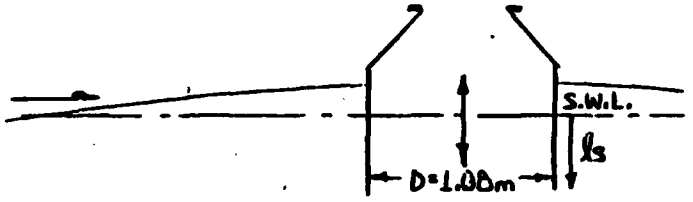

DATE	RUN	CHAMBER TOP OPENING		f_w (Hz)	DIMENSIONLESS FREQUENCY	Hi (IN.)	Hc (IN.)	Hc/Hi	OBSERVATIONS
		DIAMETER (IN.)	% OF BOTTOM						
15 DEC81	20	3.0 IN.	0.5	.325	0.678	4.85	2.99	.62	
"	21	"	0.5	.604	1.26	6.96	1.20	.17	
"	22	"	0.5	.815	1.70	6.26	0.74	.12	
26JAN82	1	SECURED TURBINE		.301	0.628	3.7	3.7	1.0	
"	2	"	"	.404	0.842	5.2	5.1	.98	
"	3	"	"	.455	0.949	5.0	4.5	.90	AIR FLOW APX. 210 FPM
"	4	"	"	.550	1.15	5.8	4.8	.83	
"	5	"	"	.674	1.41	6.3	3.3	.52	SONIC DROP-OUTS
"	6	"	"	.755	1.57	6.0	1.8	.30	SONIC DROP OUTS
"	7	FREE SPINNING TURBINE		.331	0.690	4.2	4.2	1.0	
"	8	"	"	.434	0.905	5.7	5.15	0.90	
"	9	"	"	.521	1.09	5.4	4.5	.83	AIR FLOW APX. 180 FPM
"	10	"	"	.605	1.26	6.1	2.9	.48	SUPERPOSITION OF UNSEEN WAVES
"	11	"	"	.709	1.48	6.3	2.4	.38	

APPENDIX IX: Typical Pneumatic Device Strip Chart Record

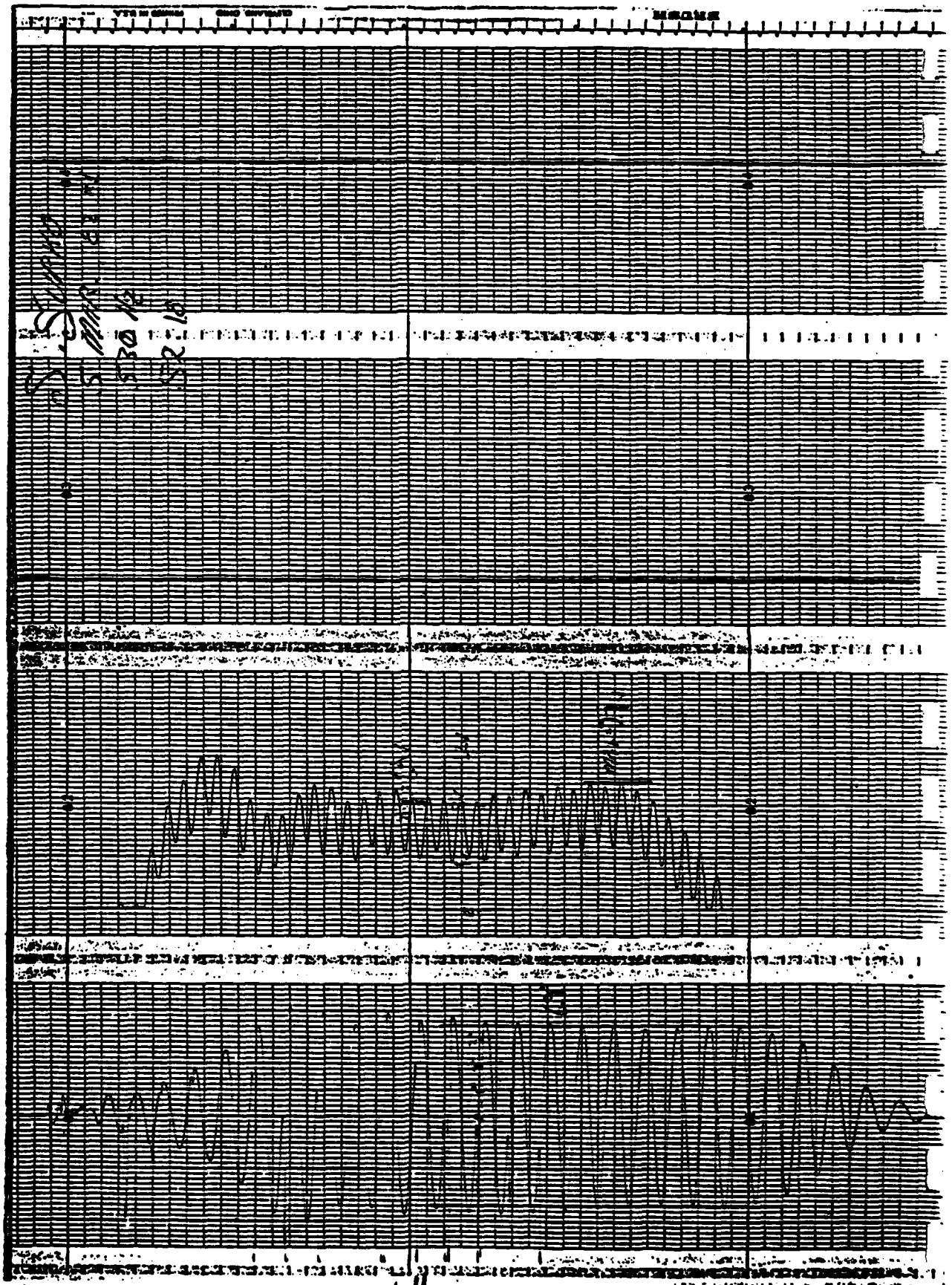

APPENDIX X: Phase Lag of the System as Observed Through the Capture Chamber's Window

APPENDIX XI: Pneumatic Wave Energy Conversion Device Data From Monochromatic Wave Analysis

PNEUMATIC WAVE ENERGY CONVERSION

LENGTH OF SUBMERGENCE (l_s) = 18" WAVE FREQUENCY ~ f_{ω}

INCIDENT WAVE HEIGHT ~ Hi

WAVE GROUP VELOCITY, $C_g = \frac{1}{2}$ WAVE VELOCITY, C, IN DEEP WATER $= \frac{1}{2}\left(\frac{gT}{2\pi}\right)$

INCIDENT WAVE POWER $= \frac{\rho g (Hi)^2 C_g}{8}$ · CAPTURE CHAMBER BOTTOM DIAMETER

GENERATED POWER $= \frac{V^2}{R}$ WHERE GENERATOR LOAD RESISTANCE, R = 7Ω

EFFICIENCY = (AVG. GENERATED POWER / INCIDENT WAVE POWER) * 100 = η

DATE	RUN	f_{ω} (Hz) (GATE SETTING)	GEAR RATIO TURBINE : GENERATOR	Hi (IN.)	Hi (m)	Hi/D	INCIDENT WAVE POWER (WATTS)	GENERATED VOLTAGE AVG.	GENERATED VOLTAGE MAX.	AVERAGE GENERATED POWER (WATTS)	η	OBSERVATIONS
25 FEB 82	1	.530 (.940)	42:28	6.8	.173	.160	58	5.1	6.8	3.7	6.4	
"	2	.530 (.940)	42:28	6.8	.173	.160	58	5.0	6.7	3.6	6.2	DIFFERENT CHAIN TENSION
"	3	.530 (.940)	42:34	6.7	.170	.157	56	4.1	5.8	2.4	4.3	
"	4	.530 (.940)	42:22	6.7	.168	.156	55	5.0	7.1	3.6	6.5	
"	5	.530 (.940)	42:18	6.7	.170	.157	56	4.3	7.2	2.6	4.6	
"	6	.530 (.940)	52:34	6.8	.173	.160	58	5.1	6.7	3.7	6.4	
"	7	.530 (.940)	52:28	6.8	.173	.160	58	5.0	7.0	3.6	6.2	
"	8	.530 (.940)	52:22	6.8	.173	.160	58	3.6	6.6	1.9	3.3	
26 FEB 82	1	.530 (.600)	42:28	4.5	.114	.106	25	1.1	2.2	.17	0.7	
"	2	.530 (.900)	42:28	6.6	.168	.156	55	4.2	6.4	2.5	4.6	
"	3	.530 (.750)	42:28	5.7	.145	.134	41	2.4	4.2	.82	2.0	
"	4	.530 (.650)	42:28	6.3	.160	.148	50	4.0	6.2	2.3	4.6	
"	5	.530 (1.00)	42:28	7.3	.185	.171	67	5.5	7.8	4.3	6.4	
"	6	.530 (1.100)	42:28	8.0	.203	.188	80	6.6	8.7	6.2	7.8	

PNEUMATIC WAVE ENERGY CONVERSION

LENGTH OF SUBMERGENCE (l_s) = 18" WAVE FREQUENCY ~ f_w

INCIDENT WAVE HEIGHT ~ Hi

WAVE GROUP VELOCITY, $C_g = \frac{1}{2}$ WAVE VELOCITY, C, IN DEEP WATER $= \frac{1}{2}\left(\frac{gT}{2\pi}\right)$

INCIDENT WAVE POWER $= \frac{\rho g (Hi)^2 C_g}{8}$ · CAPTURE CHAMBER BOTTOM DIAMETER

GENERATED POWER $= \frac{V^2}{R}$ WHERE GENERATOR LOAD RESISTANCE, R = 7Ω

EFFICIENCY = (AVG. GENERATED POWER / INCIDENT WAVE POWER) * 100 = η

DATE	RUN	f_w (Hz) & (GEAR-SETTING)	GEAR RATIO TURBINE : GENERATOR	Hi (IN.)	Hi (m)	Hi/D	INCIDENT WAVE POWER (WATTS)	GENERATED VOLTAGE AVG.	GENERATED VOLTAGE MAX.	AVERAGE GENERATED POWER (WATTS)	η	OBSERVATIONS
28FEB82	7	.530 (0.150)	42:28	7.1	.180	.167	63	4.8	6.7	3.3	5.2	INCONSISTENT ~ NOT USED IN LATER CALCULATIONS
"	8	.530 (1.150)	42:28	8.5	.216	.200	91	7.3	9.4	7.6	8.4	
"	9	.530 (1.250)	42:28	9.2	.234	.217	107	8.3	10.3	9.8	9.2	
"	10	.530 (1.300)	42:28	9.6	.244	.226	116	9.1	11.4	11.8	10.2	
"	11	.530 (1.400)	42:28	10.0	.254	.235	126	9.8	12.5	13.7	10.9	
"	12	.530 (1.500)	42:28	10.3	.262	.243	134	10.8	12.9	16.7	12.5	
"	13	.530 (.600)	42:28	5.9	.150	.139	44	3.9	5.5	1.7	3.9	
"	14	.530 (1.600)	42:28	11.0	.279	.258	152	11.5	13.9	18.9	12.4	
"	15	.530 (1.800)	42:28	12.0	.305	.282	182	11.9	13.9	20.2	11.1	
"	16	.530 (1.900)	42:28	12.8	.325	.301	206	12.9	15.4	23.8	11.6	
"	17	.530 (1.700)	42:28	11.6	.295	.273	170	11.7	13.8	19.6	11.5	
"	18	.530 (2.00)	42:28	13.2	.335	.310	219	13.7	16.2	26.8	12.2	
"	19	.530 (1.850)	42:28	12.1	.307	.284	184	12.9	15.4	23.8	12.9	
1MARCH82	1	.530 (1.650)	42:28	10.1	.257	.238	129	10.5	—	15.8	12.2	

PNEUMATIC WAVE ENERGY CONVERSION

LENGTH OF SUBMERGENCE (l_s) = 18" WAVE FREQUENCY ~ f_w

INCIDENT WAVE HEIGHT ~ Hi

WAVE GROUP VELOCITY, $C_g = \frac{1}{2}$ WAVE VELOCITY, C, IN DEEP WATER $= \frac{1}{2}\left(\frac{gT}{2\pi}\right)$

INCIDENT WAVE POWER $= \frac{\rho g (Hi)^2 C_g}{8}$ · CAPTURE CHAMBER BOTTOM DIAMETER

GENERATED POWER $= \frac{V^2}{R}$ WHERE GENERATOR LOAD RESISTANCE, R = 7Ω

EFFICIENCY = (AVG. GENERATED POWER / INCIDENT WAVE POWER) * 100 = η

DATE	RUN	f_w (Hz) (RPM-SETTING)	GEAR RATIO TURBINE : GENERATOR	Hi (IN.)	Hi (m)	Hi/D	INCIDENT WAVE POWER (WATTS)	GENERATED VOLTAGE AVG.	GENERATED VOLTAGE MAX.	AVERAGE GENERATED POWER (WATTS)	η	OBSERVATIONS
1 MARCH 82	2	.530 (1.800)	42:28	10.7	.272	.252	144	11.2	14.2	17.9	12.4	
"	3	.530 (2.300)	42:28	13.7	.348	.322	236	14.4	18.	29.6	12.5	THE WAVE FORCE CAUSED THE CHAMBER TO MOVE ABOUT 1/2"
"	4	.530 (2.400)	42:28	14.0	.356	.330	247	14.5	18.1	30.0	12.2	
"	5	.530 (1.950)	42:28	12.4	.315	.292	194	12.4	15.2	22.0	11.3	
"	6	.530 (1.950)	42:28	12.4	.315	.292	194	12.4	15.2	22.0	11.3	
"	7	.530 (1.892)	42:28	12.	.305	.282	182	11.8	14.2	19.9	10.9	
"	8	.530 (1.650)	42:28	10.9	.277	.256	150	10.5	13.3	15.8	10.5	
2 MARCH 82	1	.530 (1.540)	42:28	9.9	.251	.232	123	9.5	12	12.9	10.5	
"	2	.530 (1.540)	42:28	9.8	.249	.231	121	9.2	11.4	12.1	10.0	
"	3	.530 (1.500)	42:34	10.1	.257	.238	129	9.2	11.2	12.1	9.4	
"	4	.530 (1.500)	42:34	10.0	.254	.235	126	9.2	11.0	12.1	9.6	
"	5	.530 (1.560)	42:28	10.0	.254	.235	126	9.6	12.4	13.2	10.4	
"	6	.530 (1.500)	42:22	10.0	.254	.235	126	10.6	13.6	16.1	12.8	
"	7	.530 (1.560)	42:18	10.0	.254	.235	126	11.2	14.4	17.9	14.2	

PNEUMATIC WAVE ENERGY CONVERSION

LENGTH OF SUBMERGENCE (l_s) = 18" WAVE FREQUENCY ~ f_w

INCIDENT WAVE HEIGHT ~ Hi

WAVE GROUP VELOCITY, C_g = ½ WAVE VELOCITY, C, IN DEEP WATER = $\frac{1}{2}\left(\frac{gT}{2\pi}\right)$

INCIDENT WAVE POWER = $\frac{\rho g (Hi)^2 C_g}{8}$ · CAPTURE CHAMBER BOTTOM DIAMETER

GENERATED POWER = $\frac{V^2}{R}$ WHERE GENERATOR LOAD RESISTANCE, R = 7Ω

EFFICIENCY = (AVG. GENERATED POWER / INCIDENT WAVE POWER) * 100 = %

DATE	RUN	f_w (Hz) & (GAIN-SETTING)	GEAR RATIO TURBINE : GENERATOR	Hi (IN.)	Hi (m)	Hi/D	INCIDENT WAVE POWER (WATTS)	GENERATED VOLTAGE AVG.	GENERATED VOLTAGE MAX.	AVERAGE GENERATED POWER (WATTS)	%	OBSERVATIONS
2 MARCH 1982	8	.530 (1.500)	42 : 14	10.0	.254	.235	126	11.8	15.6	19.9	15.8	
"	9	.530 (1.500)	52 : 34	10.0	.254	.235	126	10.1	12.4	14.6	11.6	
"	10	.530 (1.500)	52 : 28	10.0	.254	.235	126	12.2	14.9	21.3	16.9	INCONSISTENT - NOT USED IN LATER CALCULATIONS
"	11	.530 (1.500)	52 : 22	10.0	.254	.235	126	12.0	15.6	20.6	16.3	
"	12	.530 (1.500)	52 : 18	10.0	.254	.235	126	12.2	16.0	21.3	16.9	
"	13	.530 (1.500)	52 : 14	10.0	.254	.235	126	9.8	15.5	13.7	10.9	
"	14	.530 (1.500)	52 : 28	10.0	.254	.235	126	10.4	12.8	15.5	12.3	
"	15	.530 (1.300)	52 : 28	8.9	.226	.209	100	9.0	11.5	11.6	11.6	
"	16	.530 (1.260)	52 : 28	8.0	.203	.188	80	6.8	9.8	6.6	8.3	
"	17	.530 (1.260)	52 : 22	8.0	.203	.188	80	8.5	11.8	10.3	12.9	
"	18	.530 (1.260)	52 : 18	8.0	.203	.188	80	6.8	11.0	6.6	8.3	
"	19	.530 (1.260)	52 : 14	8.0	.203	.188	80	7.0	11.6	7.0	8.8	
"	20	.530 (1.260)	52 : 34	8.0	.203	.188	80	5.6	8.1	4.5	5.6	CHAIN JUMPED OFF
"	21	.530 (1.260)	42 : 34	8.0	.203	.188	80	7.5	9.0	8.0	10.0	INCONSISTENT - RERUN THIS WAVE

PNEUMATIC WAVE ENERGY CONVERSION

LENGTH OF SUBMERGENCE (l_s) = 18" WAVE FREQUENCY ~ f_w

INCIDENT WAVE HEIGHT ~ Hi

WAVE GROUP VELOCITY, $C_g = \frac{1}{2}$ WAVE VELOCITY, C, IN DEEP WATER $= \frac{1}{2}\left(\frac{gT}{2\pi}\right)$

INCIDENT WAVE POWER $= \frac{\rho g (Hi)^2 C_g}{8}$ · CAPTURE CHAMBER BOTTOM DIAMETER

GENERATED POWER $= \frac{V^2}{R}$ WHERE GENERATOR LOAD RESISTANCE, R = 7 Ω

EFFICIENCY = (AVG. GENERATED POWER / INCIDENT WAVE POWER) * 100 = η

DATE	RUN	f_w (Hz) & (GAIN-SETTING)	GEAR RATIO TURBINE : GENERATOR	Hi (IN.)	Hi (m)	Hi/D	INCIDENT WAVE POWER (WATTS)	GENERATED VOLTAGE AVG.	GENERATED VOLTAGE MAX.	AVERAGE GENERATED POWER (WATTS)	η	OBSERVATIONS
2 MARCH 1982	22	.530 (1.200)	42:28	8.0	.203	.188	80	7.5	10.0	8.0	10.0	INCONSISTENT - RE-RUN
"	23	.530 (1.200)	42:28	8.0	.203	.188	80	8.0	10.0	9.1	11.4	THESE WAVES
3 MARCH 1982	1	.530 (1.150)	42:28	8.0	.203	.188	80	6.8	9.5	6.6	8.3	
"	2	.530 (1.150)	42:34	8.0	.203	.188	80	4.7	6.5	3.2	4.0	
"	3	.530 (1.150)	42:22	8.0	.203	.188	80	6.4	9.5	5.9	7.4	
"	4	.530 (1.150)	42:18	8.0	.203	.188	80	7.2	10.8	7.4	9.3	
"	5	.530 (1.150)	42:14	8.0	.203	.188	80	6.3	——	5.7	7.2	
"	6	.530 (1.150)	52:34	8.0	.203	.188	80	6.0	8.5	5.1	6.4	CHAIN SLIPPED OFF
"	7	.530 (1.150)	52:28	8.0	.203	.188	80	6.4	9.5	5.9	7.4	
"	8	.530 (1.150)	52:22	8.0	.203	.188	80	7.6	11.0	8.3	10.4	
"	9	.530 (1.150)	52:18	8.0	.203	.188	80	7.3	11.2	7.6	9.5	
"	10	.530 (1.150)	52:14	8.0	.203	.188	80	7.0	10.5	7.0	8.8	
"	11	.530 (1.150)	42:34	8.0	.203	.188	80	5.3	7.2	4.0	5.0	
"	12	.530 (1.150)	52:34	8.0	.203	.188	80	4.5	6.4	2.9	3.6	CHAIN ONLY KEPT ON BY MY HANDS

PNEUMATIC WAVE ENERGY CONVERSION

LENGTH OF SUBMERGENCE (l_s) = 18" WAVE FREQUENCY ~ f_{cw}

INCIDENT WAVE HEIGHT ~ Hi

WAVE GROUP VELOCITY, $C_g = \frac{1}{2}$ WAVE VELOCITY, C, IN DEEP WATER $= \frac{1}{2}\left(\frac{gT}{2\pi}\right)$

INCIDENT WAVE POWER $= \frac{\rho g (Hi)^2 C_g}{8}$ · CAPTURE CHAMBER BOTTOM DIAMETER

GENERATED POWER $= \frac{V^2}{R}$ WHERE GENERATOR LOAD RESISTANCE, R = 7Ω

EFFICIENCY = (AVG. GENERATED POWER / INCIDENT WAVE POWER) * 100 = η

DATE	RUN	f_{cw} (Hz) (GRAN-SETTING)	GEAR RATIO TURBINE : GENERATOR	Hi (IN.)	Hi (m)	Hi/D	INCIDENT WAVE POWER (WATTS)	GENERATED VOLTAGE AVG.	GENERATED VOLTAGE MAX.	AVERAGE GENERATED POWER (WATTS)	η	OBSERVATIONS
3 MARCH 1982	13	.530 (1.150)	42:14	8.0	.203	.188	80	6.6	10.4	6.2	7.8	
"	14	.530 (1.150)	42:28	8.0	.203	.188	80	6.6	8.9	6.2	7.8	
4 MARCH 1982	1	.536 (.690)	52:18	4.4	.112	.104	25	0	1.0	0	0	INCONSISTENT: CALIBRATION OFF
"	2	.534 (1.300)	52:18	8.8	.224	.207	98	4.5	6.3	2.9	3.0	AND/OR CHAIN TOO TIGHT
"	3	.534 (1.600)	52:18	10.0	.254	.235	126	6.5	8.3	6.0	4.8	DATA NOT USED IN LATER CALCULATIONS
"	4	.530 (1.900)	52:18	11.4	.290	.269	164	18	—	46.3	28.2	
"	5	.530 (1.900)	52:18	11.2	.284	.263	157	17.8	22	45.3	28.9	
"	6	.530 (1.700)	52:18	10.7	.272	.252	144	15.5	19.3	34.3	23.8	
"	7	.530 (1.500)	52:18	9.6	.244	.226	116	13	17	24.1	20.8	
"	8	.530 (1.300)	52:18	8.4	213	.197	89	10.1	14	14.6	16.4	
"	9	.530 (1.100)	52:18	7.2	.183	.169	65	7.2	11.0	7.4	11.4	
"	10	.530 (.900)	52:18	5.8	.147	.136	42	3.9	7.2	2.17	5.2	
"	11	.530 (.750)	52:18	5.2	.132	.122	34	1.0	3.8	.14	0.4	
"	12	.530 (1.000)	52:18	7.0	.178	.165	62	5.6	9.4	4.5	7.3	

PNEUMATIC WAVE ENERGY CONVERSION

LENGTH OF SUBMERGENCE (l_s) = 18" WAVE FREQUENCY ~ f_{cw}

INCIDENT WAVE HEIGHT ~ Hi

WAVE GROUP VELOCITY, $C_g = \frac{1}{2}$ WAVE VELOCITY, C, IN DEEP WATER $= \frac{1}{2}\left(\frac{gT}{2\pi}\right)$

INCIDENT WAVE POWER $= \frac{\rho g (Hi)^2 C_g}{8}$ • CAPTURE CHAMBER BOTTOM DIAMETER

GENERATED POWER $= \frac{V^2}{R}$ WHERE GENERATOR LOAD RESISTANCE, R = 7 Ω

EFFICIENCY = (AVG. GENERATED POWER / INCIDENT WAVE POWER) * 100 = η

DATE	RUN	f_{cw} (Hz) (CRANK SETTING)	GEAR RATIO TURBINE : GENERATOR	Hi (IN.)	Hi (m)	Hi/D	INCIDENT WAVE POWER (WATTS)	GENERATED VOLTAGE AVG.	GENERATED VOLTAGE MAX.	AVERAGE GENERATED POWER (WATTS)	η	OBSERVATIONS
4 MARCH 1982	13	.530 (1.200)	52:18	8.0	.203	.188	80	8.5	12.2	10.3	12.9	
"	14	.530 (2.100)	52:18	12.5	.318	.294	197	21.5	26	66.0	33.5	
"	15	.530 (2.250)	52:18	13	.330	.306	212	20.5	25	60.0	28.3	
5 MARCH 1982	1	.530 (1.040)	52:18	6.9	.175	.162	60	6.4	9.7	5.9	9.8	
"	2	.530 (2.400)	52:18	13.9	.353	.327	243	24.6	30.0	86.5	35.6	
"	3	.5300 (1.250)	52:18	8.3	.211	.195	87	10.8	14.2	16.7	19.2	

APPENDIX XII: Pneumatic Device Performance in a Random Sea

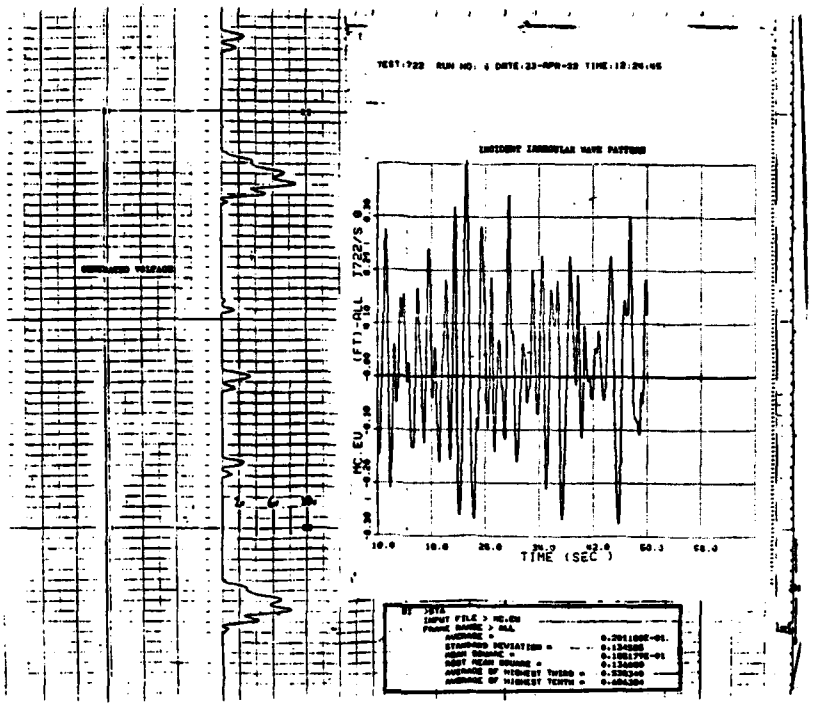

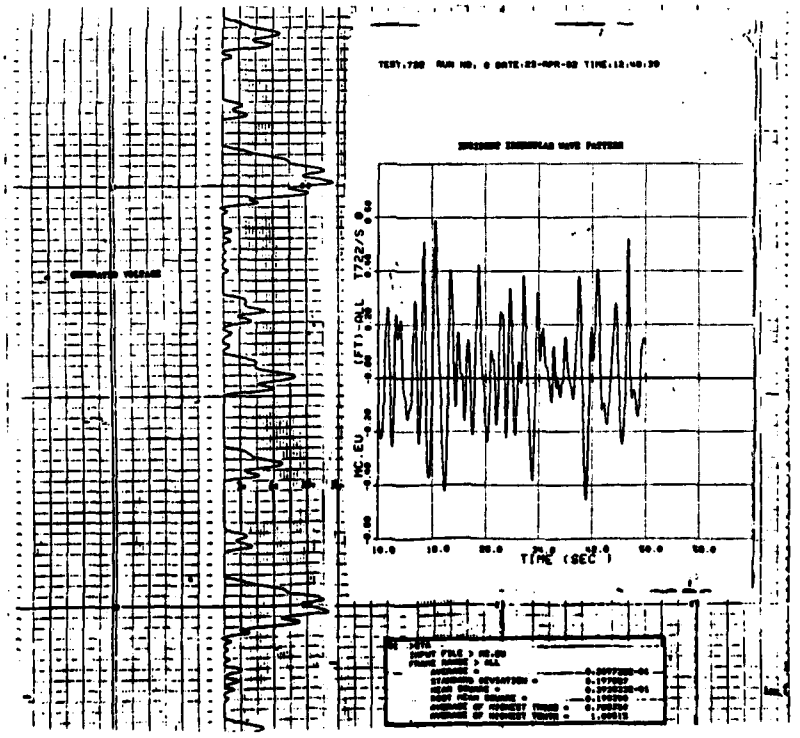

UNCLASSIFIED

SECURITY CLASSIFICATION OF THIS PAGE (When Data Entered)

REPORT DOCUMENTATION PAGE	READ INSTRUCTIONS BEFORE COMPLETING FORM
1. REPORT NUMBER: U.S.N.A. - TSPR; no. 120 (1982)	2. GOVT ACCESSION NO.: AD-A
3. RECIPIENT'S CATALOG NUMBER	
4. TITLE (and Subtitle): PERFORMANCE OPTIMIZATION OF A PNEUMATIC WAVE ENERGY CONVERSION DEVICE.	5. TYPE OF REPORT & PERIOD COVERED: Final: 1981/1982
	6. PERFORMING ORG. REPORT NUMBER
7. AUTHOR(s): Surko, Stephen W.	8. CONTRACT OR GRANT NUMBER(s)
9. PERFORMING ORGANIZATION NAME AND ADDRESS: United States Naval Academy, Annapolis.	10. PROGRAM ELEMENT, PROJECT, TASK AREA & WORK UNIT NUMBERS
11. CONTROLLING OFFICE NAME AND ADDRESS: United States Naval Academy, Annapolis.	12. REPORT DATE: 26 August 1982
	13. NUMBER OF PAGES: 73
14. MONITORING AGENCY NAME & ADDRESS (if different from Controlling Office)	15. SECURITY CLASS. (of this report): UNCLASSIFIED
	15a. DECLASSIFICATION/DOWNGRADING SCHEDULE

16. DISTRIBUTION STATEMENT (of this Report)

This document has been approved for public release; its distribution is UNLIMITED.

17. DISTRIBUTION STATEMENT (of the abstract entered in Block 20, if different from Report)

This document has been approved for public release; its distribution is UNLIMITED.

18. SUPPLEMENTARY NOTES

Accepted by the U. S. Trident Scholar Committee.

19. KEY WORDS (Continue on reverse side if necessary and identify by block number)

Ocean wave power.
Water-power electric plants.

20. ABSTRACT (Continue on reverse side if necessary and identify by block number)

The performance of a pneumatic wave energy conversion device was optimized by developing resonance within the device's oscillating water column and impedance matching the system.

The pneumatic device investigated was one quarter the size of prototype recently constructed. Within its capture chamber is a column of water which is excited by the incident waves. The capture chamber has a bottom opening so that the system is omni directional. As the water column oscillates it forces

(OVER)

air through a special counter-rotating axial flow turbine developed by Professor M. McCormick which always drives an output shaft in the same direction regardless of the direction of air flow. The internal water column oscillations obey the equation of motion.

In accordance with the equation of motion the author was able to control the internal frequency of oscillation to develop resonance with the incident waves. This resonant condition served to strengthen the oscillations of the water column within the capture chamber and to attract additional wave energy through an effect known as "antenna focusing." In this study, resonance was achieved by varing the length of submergence of the capture chamber.

A special low-rpm generator was purchased to convert the turbine revolutions into usable power. A linkage system consisting of a 10-speed bicycle's chain and gears was modified to transfer the turbine rpm to the generator, and the generator load to the turbine, to impedance match the system. The various gear ratios allowed the system to be impedance matched for different incident waves.

During monochromatic wave testing a maximum efficiency of 35.6 percent was achieved, at a developed power of 86.5 watts. Efficiencies dropped off rapidly in wave conditions of less incident power.

During the brief period of random sea wave testing the efficiency dropped as low as .6 percent, as compared to 10 percent for a similar monochromatic wave. There appear to be several means of improving the random sea performance. The use of a flywheel to smooth out the turbine response to the varying incident waves was found to offer promise, although the one which the author added on to the turbine was too small to have a significant effect. If, instead of using the submergence length, air compressibility is used to control the internal water column frequency then response to varying incident waves could be swift to maintain resonance. A control system is necessary to adjust the air compressibility and the system load to maintain optimum performance in ocean wave energy conversion revealed by the brief period of random sea testing the great potential for pneumatic wave energy conversion remains.

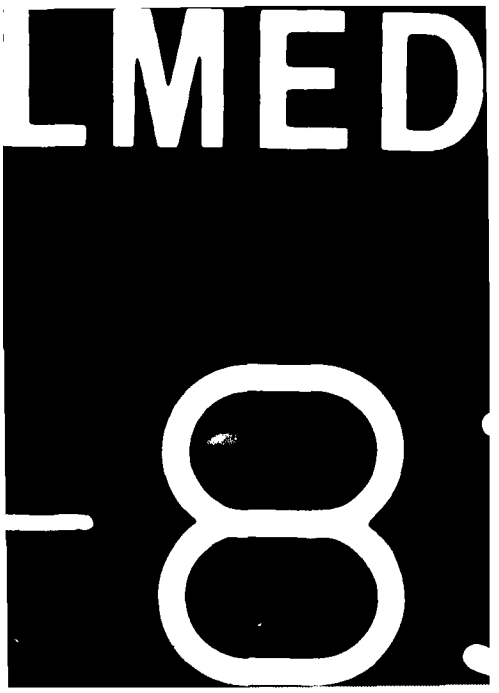
LMED
8